

Motives of melonic graphs

Paolo Aluffi, Matilde Marcolli, and Waleed Qaisar

Abstract. We investigate recursive relations for the Grothendieck classes of the affine graph hypersurface complements of melonic graphs. We compute these classes explicitly for several families of melonic graphs, focusing on the case of graphs with valence-4 internal vertices, relevant to CTKT tensor models. The results hint at a complex and interesting structure in terms of divisibility relations or nontrivial relations between classes of graphs in different families. Using the recursive relations, we prove that the Grothendieck classes of all melonic graphs are positive as polynomials in the class of the moduli space $\mathcal{M}_{0,4}$. We also conjecture that the corresponding polynomials are *log-concave*, on the basis of hundreds of explicit computations.

Contents

1. Introduction	503
2. Melonic graphs	509
3. Grothendieck classes of melonic graphs	517
4. Explicit computations, I	529
5. Explicit computations, II	533
6. Vacua	537
7. Proofs	544
References	552

1. Introduction

In this paper, we obtain a recursive formula for the Grothendieck classes (virtual motives) of the graph hypersurfaces associated to the melon-tadpole graphs. This provides a recursively constructed family of mixed-Tate motives, which includes the motives associated to the leading melonic terms of certain bosonic tensor models.

2020 Mathematics Subject Classification. Primary 14C15; Secondary 81T15.

Keywords. Tensor models, melonic graphs, graph hypersurfaces, Grothendieck ring of varieties, log concavity.

Our motivation in considering the behavior of the motives of melon and melon-tadpole graphs comes from the fact that several interesting physical models are dominated in the large N limit by melonic graphs. This is the case for SYK models (see [14] for a rigorous diagrammatic proof), as well as in group field theory (see, for instance, [7]) and tensor models [12, 18, 22, 25], which include generalizations of the SYK models (see for instance [19, 35]).

1.1. Graph polynomials and CTKT models

The graph polynomials that one expects to find when representing amplitudes in Feynman parametric form in the setting of group field theory and tensor models are usually of the form described in [20] or [34]. The Tanasa graph polynomials of [34] are generalizations of the Bollobás–Riordan polynomial that satisfy the deletion-contraction relation. Similarly, the Gurau polynomials of [20] also satisfy a deletion-contraction relation. The motives of hypersurfaces associated to these polynomials may be, in principle, amenable to the kind of algebro-geometric techniques discussed in [4], which we rely on in this paper, but in a form more similar to the case of the Potts models we analyzed in [5]. However, the computation of the Grothendieck class we obtain here relies essentially on the recursive form of the Grothendieck class for splitting an edge and for replacing an edge by a number of parallel edges, obtained in [4]. These formulas do not have a simple counterpart for the case of the Potts models and other graph polynomials with deletion-contraction. This means that a more general computation of the polynomials of [20] or [34] probably requires a much more thorough analysis and would not be an immediate generalization of the argument presented here. Other parametric realizations of tensor models, such as [9], do not even satisfy a deletion-contraction relation, hence they cannot be addressed via the method used in [4] and in this paper.

The case we focus on here, however, is simpler and involves the usual graph hypersurfaces associated to the Kirchhoff–Symanzik polynomial of the graph for a massless scalar theory. These are relevant to tensor models in the case of the melonic sector of the CTKT models. We briefly recall below the setting used in [10] that motivates the computations we present in this paper. The case of the graph polynomials of [20] or [34] will be left to a future investigation. Note that, if a similar argument can be applied to such polynomials, or to the massive melonic graphs, one does not expect to obtain a family of motives with the mixed-Tate property, since it is known that already for small graphs in such families the mixed-Tate property fails, see [11, 31]. Thus, the mixed-Tate property is certainly specific to the case of the massless Kirchhoff–Symanzik polynomial.

1.2. CTKT models and melonic Feynman graphs

We focus here on the modified version of the $O(N)^3$ model by Klebanov and Taronpolisky [27] considered in [10], which generalizes the zero-dimensional version of [15]. These models are referred to in [10] as CTKT models, and we will maintain the same terminology here.

We recall the following setting from [10]. One considers a real rank three tensor field $\phi_{\mathbf{a}}(x)$, with $\mathbf{a} = (a_1, a_2, a_3)$ that transforms under $O(N)^3$, with action functional

$$\begin{aligned}
 \mathcal{S}[\phi] &= \frac{1}{2} \int \phi_{\mathbf{a}}(x)(-\Delta)\phi_{\mathbf{a}}(x) \text{dvol}(x) + \mathcal{S}^{\text{int}}[\phi], \\
 \mathcal{S}^{\text{int}}[\phi] &= \frac{m^2}{2} \int \phi_{\mathbf{a}}(x)\delta_{\mathbf{ab}}\phi_{\mathbf{b}}(x) \text{dvol}(x) \\
 &\quad + \frac{\lambda_t}{4N^{3/2}} \int \delta_{\mathbf{abcd}}^t \phi_{\mathbf{a}}(x)\phi_{\mathbf{b}}(x)\phi_{\mathbf{c}}(x)\phi_{\mathbf{d}}(x) \text{dvol}(x) \\
 &\quad + \int \left(\frac{\lambda_p}{4N^2} \delta_{\mathbf{ab;cd}}^p + \frac{\lambda_d}{4N^3} \delta_{\mathbf{ab;cd}}^d \right) \phi_{\mathbf{a}}(x)\phi_{\mathbf{b}}(x)\phi_{\mathbf{c}}(x)\phi_{\mathbf{d}}(x) \text{dvol}(x)
 \end{aligned}
 \tag{1.1}$$

with $\Delta = \partial_{\mu}\partial^{\mu}$ and with overlap with notation of subscript d .

$$\begin{aligned}
 \delta_{\mathbf{abcd}}^t &= \delta_{a_1 b_1} \delta_{c_1 d_1} \delta_{a_2 c_2} \delta_{b_2 d_2} \delta_{a_3 d_3} \delta_{b_3 c_3}, & \delta_{\mathbf{ab}} &= \prod_i \delta_{a_i, b_i}, \\
 \delta_{\mathbf{ab;cd}}^p &= \frac{1}{3} \sum_i \delta_{a_i c_i} \delta_{b_i d_i} \prod_{i \neq j} \delta_{a_j b_j} \delta_{c_j d_j}, & \delta_{\mathbf{ab;cd}}^d &= \delta_{\mathbf{ab}} \delta_{\mathbf{cd}}.
 \end{aligned}$$

The labels t, p, d distinguish the tetrahedron, pillow, and double-trace patterns of contraction. When edges are colored (red, green, or blue) according to the values of the tensor indices in $\{1, 2, 3\}$, these different quartic terms correspond to the graphs of Figure 1 (with three different choices of the pillow contraction depending on the color of the vertical edge).

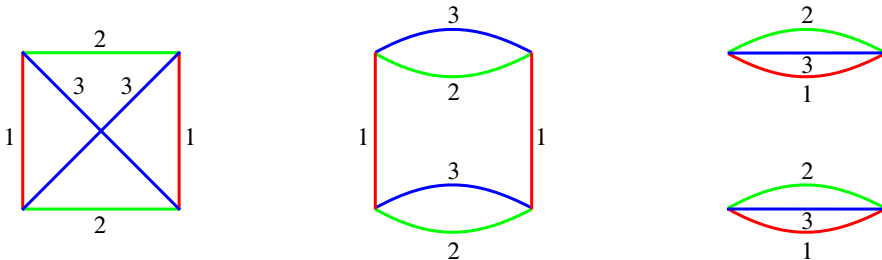


Figure 1. Tetrahedron, pillow, and double-trace contractions in CTKT models [10].

When one computes the contributions to the expansion at leading order in $1/N$ and all orders in the coupling constants, this is usually done using the 4-colored graphs expansion of tensor models [13, 21, 24] with 3-colored graphs (bubbles) for the different interaction terms as mentioned above and another color for the propagators connecting these 3-colored bubbles. However, as shown in [10], it is possible to also consider an expansion in ordinary Feynman graphs, which are obtained by shrinking all the bubbles to points. The free energy of the model is written in [10] in the form of a sum over connected vacuum 4-colored graphs with labelled tensor vertices,

$$\mathcal{F} = \sum_G N^{F - \frac{3}{2}n_t - 2n_p - 3n_d} \frac{\lambda_t^{n_t}}{n_t! 4^{n_t}} \frac{\lambda_p^{n_p}}{n_p! 12^{n_p}} \frac{\lambda_d^{n_d}}{n_d! 4^{n_d}} (-1)^{n_t + n_p + n_d + 1} \mathbb{A}(G),$$

with $n_t(G)$, $n_p(G)$, and $n_d(G)$ the number of tetrahedral, pillow, and double-trace bubbles, respectively, and $F(G)$ the number of faces and with $\mathbb{A}(G)$ the amplitude of G written in terms of edge propagators (see [10, §2.1]). One then replaces the 4-colored graphs G in this expansion with ordinary Feynman graphs by first replacing all the pillow and double trace bubbles with their minimal resolution in terms of tetrahedral bubbles (as in [10, Figure 3]). An ordinary Feynman graph is then obtained by replacing these bubbles by vertices. The resulting graph corresponds to a term of order zero in $1/N$ iff it is a melon-tadpole graph, that is, a graph obtained by iterated insertion of melons or tadpoles into a melon or tadpole (Figure 2). In the absence of pillows and double traces, one would obtain just melonic graphs. The amplitudes $\mathbb{A}(G)$ of the resulting ordinary melon-tadpole Feynman graphs can then be computed in the Feynman parametric form in terms of the Kirchhoff–Symanzik polynomial, as in [10]. We will not discuss here the renormalization problem for the resulting Feynman integrals, for which we refer the reader to [10]. We focus here instead on the algebro-geometric and motivic properties of these melon-tadpole Feynman integrals.

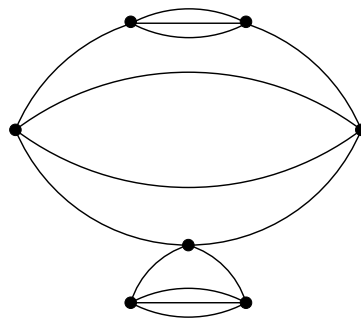


Figure 2. Melon-tadpole graphs in CTKT models [10].

From the point of view of motivic structures in quantum field theory (see [29] for a general overview), our goal here is to show that massless CTKT models are dominated by a recursively constructed family of mixed-Tate motives.

1.3. Families of melonic graphs

The melonic and melon-tadpole graphs that occur in the massless CTKT models are all constrained by the condition that all vertices have valence 4, because of the form (1.1) of the action functional. In order to study the recursive properties of the Grothendieck classes associated to these graphs, however, it is convenient to consider them as a subfamily of a larger family of graphs, which include melonic graphs with vertices of arbitrary valences.

Moreover, in the typical description of melonic graphs, one assumes that the melonic insertions are separated by edge propagators (equivalently, one performs an insertion by first splitting an edge into three edges by the insertion of two valence-two vertices and then replacing the middle edge by a number of parallel edges). Again, in our setting it is more convenient to consider these graphs as a subfamily of a larger family of melonic graphs where an edge can be split into a number of subedges and each of them replaced by a set of parallel edges. The typical case of graphs with only valence-four internal vertices and including edge propagators will guide us in the choice of examples illustrating the main recursive construction.

We also consider graphs with external edges and graphs without any external edges (vacuum bubbles). Instead of following the usual physics convention of regarding external edges as half-edges (flags), we consider them as edges with a valence-one vertex. In this setting, when considering non-vacuum graphs for the CTKT case, we will allow formal valence-one vertices (to mark the external edges) in addition to the valence-four vertices of the self-coupling interactions.

We will not treat separately the melon-tadpole graphs. Indeed, our more general class of graphs includes the operation of bisecting an edge with an intermediate vertex, and a melon-tadpole graph is simply obtained by grafting together at the vertex two melonic graphs with this operation performed on one of their edges. Since the Grothendieck classes for graphs joined at a vertex is just a product, these classes are easily derived from the ones in the family we work with.

1.4. Summary of the paper

In Section 2, we present a convenient formalism for the recursive construction of melonic graphs with arbitrary valences, and we show that a subclass of ‘reduced constructions’ always suffices. We reformulate the construction in terms of labelled

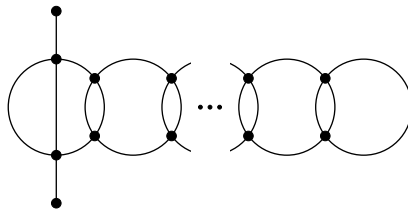
rooted trees. We then focus on the main case of interest for CTKT models, where graphs have all (internal) vertices of valence four.

In Section 3, we recall some basic facts about the Grothendieck ring of varieties, the parametric Feynman integrals, the graph hypersurfaces defined by the Kirchhoff–Symanzik polynomial, and the Grothendieck classes of the affine graph hypersurface complement. We focus on the Grothendieck class because it is universal among invariants which behave well with respect to basic set-theoretic operations. For example, the Grothendieck class determines the Hodge–Deligne numbers of the complement of the (affine) graph hypersurface, as well as the number of points of the complement over finite fields. We obtain a recursive formula for the Grothendieck class of melonic graphs with arbitrary valences. This formula can be effectively implemented in a standard symbolic manipulation system and is also useful as a tool to study general features of Grothendieck classes of melonic graphs. For example, we prove that the Grothendieck class of a melonic graph can be expressed as a polynomial with *positive* coefficients in the class \mathbb{S} of the moduli space $\mathcal{M}_{0,4}$, i.e., $\mathbb{S} = [\mathbb{P}^1 \setminus \{0, 1, \infty\}]$. Extensive computer evidence also suggests the following:

Conjecture. *The polynomial in \mathbb{S} expressing the Grothendieck class of a melonic graph is log-concave (in the sense of [33]; see Conjecture 3.1 below).*

It is well known (see [26]) that the log-concavity property often reflects some deeper underlying geometric structure, in the form of some kind of Hodge–de Rham relations. It seems likely that log-concavity of these Grothendieck classes as functions of \mathbb{S} may indeed be pointing to some richer geometric structure.

In Section 4, we focus on the case of melonic graphs with (internal) vertices of valence four, and we consider particular recursive subfamilies for which explicit generating functions can be obtained, both for vacuum bubbles and for graphs with external edges, with an explicit relation between these two cases. The generating functions in these and other cases considered in the paper were first obtained by carrying out explicit computations using the recursive formula obtained in Section 3. As an example of the type of result we obtain, consider the family consisting of graphs Γ_n of the form



with n interlocked circles. Let $P_n(u, v)$ be the *Hodge–Deligne polynomial* of the complement Z_n of the affine graph hypersurface determined by Γ_n . That is, $P_n(u, v) =$

$\sum e^{p,q} u^p v^q$, where $e^{p,q} = \sum_k (-1)^k h^{p,q}(H_c^k(Z_n))$ (see, e.g., [16]). As a consequence of Proposition 4.1, the following holds:

$$P_n(u, v) = (uv - 1)^n (uv)^{2n+1} \cdot A_n(uv - 1),$$

where the polynomial $A_n(t)$ is determined by the equality of formal power series $\sum_{n \geq 0} A_n(t) r^n = \sum_{k \geq 0} a_k(r, t)$, with

$$\sum_{k \geq 0} a_k(r, t) \frac{s^k}{k!} = e^{rs} \cos((r^2 - rt)^{\frac{1}{2}} s).$$

Alternative expressions for $A_n(t)$ are given in Section 5; in fact, the information carried by the polynomials $A_n(t)$ may be encoded in a *rational* generating function.

In Section 5, we analyze extensions of these recursive subfamilies to the more general case of arbitrary valences from the same viewpoint. Again we obtain that the corresponding Grothendieck classes are determined by rational generating functions.

In Section 6, we focus on the melonic vacuum bubbles, and we establish a general relation between their Grothendieck classes and those of associated non-vacuum graphs. We describe a procedure for studying the structure of valence-four melonic vacuum bubbles in terms of their tree structure, and we identify certain families of recursive relations in the form of ‘melonic vacuum stars’.

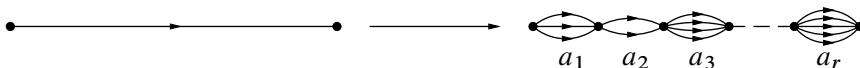
In Section 7, we give rigorous proofs of all the statements presented in the previous sections.

2. Melonic graphs

2.1. The construction of melonic graphs

A graph with two vertices and n parallel edges connecting them is variously referred to in the literature as a melon graph, a banana graph, or a sunset graph. In the spirit of botanical egalitarianism, we will use the ‘banana’ terminology when referring to these basic building blocks, and call ‘melonic’ the result of iterating the operation of replacing edges of a graph by strings of bananas. (We call this operation the ‘bananification’ of the edge.)

Thus, the basic iterative operation constructing melonic graphs is the following:



We allow arbitrary sizes a_1, \dots, a_r for the banana components. Edges ought to be directed in order to determine the order of inclusion of the bananas; in fact, this will

- (iii) k_s is an integer, $1 \leq k_s \leq |b_{p_s}|$.
- (iv) $p_s > 0$ for all $s > 1$. (By (ii), $p_1 = 0$.)
- (v) For all $t_i = ((a_1, \dots, a_{r_i}), p_i, k_i)$, $i = 1, \dots, n$, and all $j = 1, \dots, r_i$, at most a_j tuples $t_s = (b_s, p_s, k_s)$ have $p_s = i, k_s = j$.

We call n the ‘length’ of the construction.

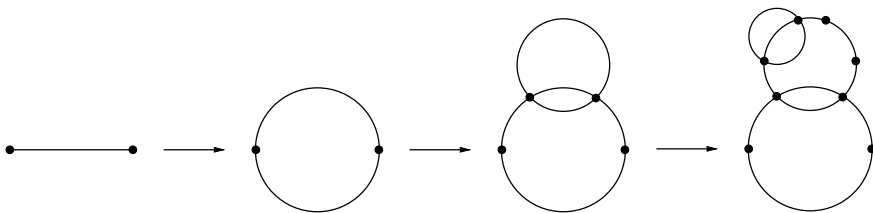
The motivation behind these requirements should be evident from the interpretation discussed above. For example, (v) expresses the constraint that the j -th banana constructed at stage i has enough edges to accommodate later replacements.

Definition 2.2. A *melonic graph* is a graph determined by a melonic construction by the procedure explained above.

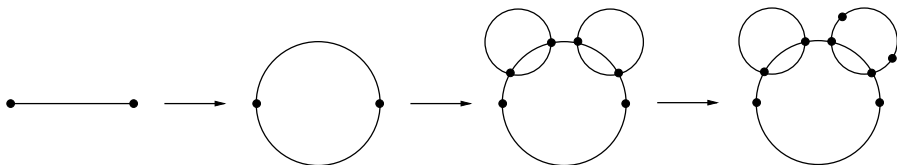
Every melonic construction determines a melonic graph up to graph isomorphism. Of course, different melonic constructions may determine the same melonic graph. We say that two constructions T', T'' are ‘equivalent’ if the resulting graphs are isomorphic.

Note that, while in the construction we have made use of an orientation of the edges, in order to list the bananas by an order of inclusion, here we consider isomorphism classes of the underlying graphs independent of the directed structure. Different choices of directed structures will lead to equivalent constructions. The Grothendieck classes we are interested in computing only depend on the underlying undirected graph.

Example 2.2. The construction $\{((2), 0, 1), ((1, 3, 1), 1, 1), ((1, 3, 1, 1, 1), 2, 2)\}$ determines a melonic graph as follows:



The construction $\{((2), 0, 1), ((1, 3, 1, 3, 1), 1, 1), ((1, 1, 1), 2, 4)\}$ produces an isomorphic graph



Also, the graph in Example 2.1 was obtained from the melonic construction

$$\{((1, 3, 5), 0, 1), ((\underline{1}, 2), 1, 2), ((1, 3, 1), 1, 3), ((\underline{2}, 3), 2, 1)\}.$$

The same graph can be obtained by the (shorter) construction

$$\{((1, 3, 5), 0, 1), ((2, 3, 2), 1, 2), ((1, 3, 1), 1, 3)\}.$$

Similarly, the second construction in Example 2.2 produces the same graph as the (longer) construction

$$\{((2), 0, 1), ((1, 3, \underline{1}), 1, 1), ((\underline{1}, 3, 1), 2, 3), ((1, 1, 1), 3, 3)\}.$$

In both cases, the shorter construction is obtained by implementing the replacement of the (single) edge in a 1-banana produced at stage s (underlined) by inserting the appropriate tuple (also underlined) directly at stage s .

Remark 2.1. In this generality, the set of all melonic graphs agrees with the set of series-parallel graphs. Indeed, series-parallel graphs can be characterized as those graphs that can be reduced to the graph K_2 by repeated application of the operations of replacement of a pair of parallel edges by a single edge and replacement of two edges joined at a degree two vertex by a single edge [17]. These are exactly reversing the operations of addition of parallel edges (bananas) and splitting of edges that form the melonic graphs. We adopted the term ‘melonic’ as it is more commonly used in the context of quantum field theory.

2.2. Reduced melonic constructions

Constructions such as Example 2.2 suggest the following definition.

Definition 2.3. We say that a construction is *reduced* if it does not prescribe the replacement of the edge of a 1-banana past stage 0.

Formally, this requirement prescribes that

- (vi) For all $t_i = ((a_1, \dots, a_{r_i}), p_i, k_i)$, $i = 1, \dots, n$: If $a_j = 1$, then $k_s \neq j$ for all s such that $p_s = i$.

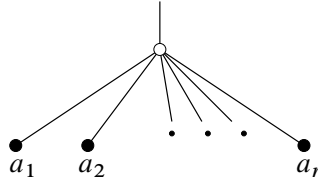
The process illustrated above—replacing 1-bananas by their descendants—may be performed on every melonic construction, and produces an equivalent reduced construction. Therefore, the following lemma is true.

Lemma 2.1. *Every melonic graph admits a reduced construction.*

Reduced constructions suffice in order to define melonic graphs, but it is important to consider non-reduced constructions as well; these may appear in intermediate steps of the recursive computation we will obtain in Section 3.

2.3. Melonic graphs and rooted trees

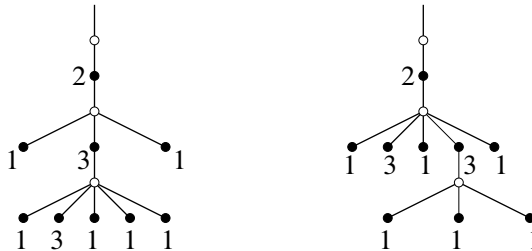
There is a convenient way to visualize a melonic construction as a labeled tree. Each tuple $((a_1, \dots, a_r), p, k)$ may be viewed as a rooted tree



with (black) leaves labeled by the integers a_i . The (white) root will be attached to the k -th leaf of the p -th tree; this grafting procedure builds a rooted tree encoding the same information as a melonic construction. Item (v) in Definition 2.1 amounts to the requirement that the valence of a (black) node labeled a is at most $a + 1$; that is, at most a ‘descending’ edges can be adjacent to such a vertex.

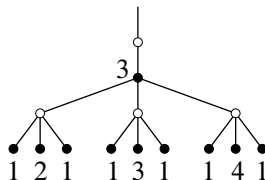
The tree corresponding to a melonic construction has one white node for each tuple in the construction; thus, the length of the melonic construction equals the number of white nodes in the corresponding tree.

Example 2.3. The rooted trees corresponding to the two melonic constructions in Example 2.2 are



As noted in Example 2.2, these non-isomorphic labeled trees determine isomorphic melonic graphs.

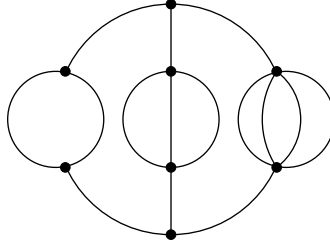
Black nodes in trees corresponding to melonic constructions may have more than one white child; in fact, the label attached to a black node indicates the maximum possible number of white children of that node. For example, the tree



corresponds to the construction

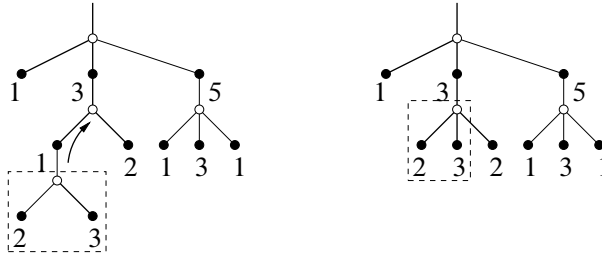
$$((3), 0, 1), ((1, 2, 1), 1, 1), ((1, 3, 1), 1, 1), ((1, 4, 1), 1, 1)$$

representing the melonic graph



No other white node could be adjacent to the black node labeled 3, since all edges of the corresponding banana support further stages of the construction.

The ‘reduced’ condition (vi) is the requirement that nodes labeled 1 necessarily be leaves. Every tree can be reduced (cf. Lemma 2.1) by ‘sliding up’ trees grafted at nodes labeled 1, as the case encountered in Example 2.1 illustrates.



We also note that the melonic graphs determined in Definition 2.2 have arbitrary vertex valences, while in a specific physical theory the valences are constrained by the terms in the action. The additional generality is needed for the recursion formula we will obtain in Section 3; we will choose families of graphs with fixed valence in most of the examples illustrating the recursion in Sections 4, 5, and 6.

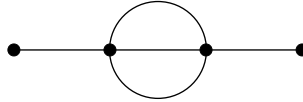
While we do not pursue explicitly this point of view in the present paper, it is an interesting question whether the generative process describing the melonic graphs can be formulated as a regular formal language. The presence of a rational generating series suggests this may be the case. More general Feynman graphs of quantum field theories can be described as a formal language involving graph grammars, see [30], which are usually in the larger class of context-free grammars.

2.4. Valence-four 2-point melonic graphs

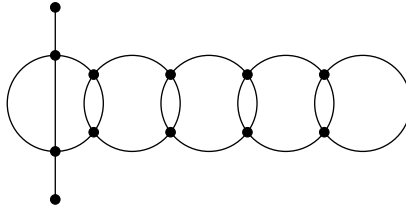
We will be especially interested in the case in which the valence of all internal vertices of the melonic graph is 4. The 4-regular melonic graphs include a class given by the 2-point melonic graphs, see for instance [23, Section 4]. These are the melonic graphs obtained starting with the graph K_2 (one edge with two end vertices) by successive insertions of pairs of vertices in an edge and replacement of the resulting middle edge by a set of three parallel edges (banana). These graphs have vertices with at most a single external momentum. The corresponding melonic constructions consist of tuples of the type

$$t_s = ((1, 3, 1), p_s, k_s),$$

where $k_s = 1, 2,$ or 3 . The building blocks of these graphs are

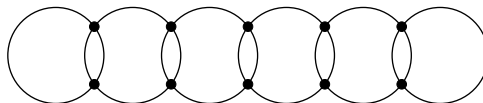


Up to equivalence, a melonic construction (t_1, \dots, t_m) with $t_s = ((1, 3, 1), p_s, k_s)$ as above is determined by the tuple $(0, p_2^\pm, \dots, p_n^\pm)$, where each p_s for $s > 1$ is marked as p_s^+ if $k_s = 2$ and p_s^- if $k_s = 1$ or 3 . For example, $(0, 1^+, 2^+, 3^+, 4^+)$ indicates that at each stage the new splitting $(1, 3, 1)$ is performed on one of the 3 parallel edges at the previous stage. The corresponding melonic graph may be drawn as follows:



2.5. 2-point melonic vacuum bubbles

We will also consider the ‘vacuum’ flavor of these constructions, in which the two external vertices are identified; for example



Definition 2.4. *Vacuum bubbles of 2-point melonic graphs are 2-point melonic graphs without valence-1 vertices.*

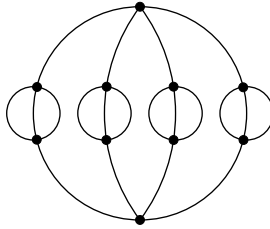
A vacuum 2-point melonic graph in which every vertex has valence 4 may be obtained by iteratively applying the basic bananification $((1, 3, 1), p_s, k_s)$ starting from a 4-banana. For example, the string of circles depicted above is produced by the construction

$$(((4), 0, 1), ((1, 3, 1), 1, 1), ((1, 3, 1), 2, 2), ((1, 3, 1), 3, 2), ((1, 3, 1), 4, 2)),$$

while the construction

$$(((4), 0, 1), ((1, 3, 1), 1, 1), ((1, 3, 1), 1, 1), ((1, 3, 1), 1, 1), ((1, 3, 1), 1, 1))$$

yields the vacuum melonic graph

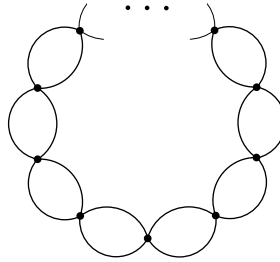


Note that all valence-4 vacuum bubbles of 2-point melonic graphs may also be constructed by starting from a 2-banana, performing iteratively the basic $(1, 3, 1)$ bananifications, and then removing the two extra valence-2 vertices produced at the beginning. Indeed, the 4-banana itself admits such a description: the melonic construction

$$(((2), 0, 1), ((1, 3, 1), 1, 1))$$

produces the 4-banana graph with two extra valence-2 vertices on one of the edges. This alternative will be convenient in our computations concerning certain families of vacuum melonic graphs in Section 6.

Remark 2.2. In this section and in the explicit examples given in the rest of the paper, we focus on 2-point melonic graphs and the associated vacuum bubble graphs, since they are the first family of melonic graphs relevant to quantum field theory due to their contribution to the 2-point function, see [23]. These do not exhaust the entire family of valence-4 graphs obtainable from the more general melonic construction discussed in the previous subsection. Melonic graphs that are not among the 2-point graphs and the corresponding vacuum bubbles include, for example, those with vertices that have two external edges. The associated melonic vacuum graphs, obtained by pairing these external edges, include graphs obtainable by our general construction but not in the list of vacuum bubbles of 2-point melonic graphs. For instance, the necklace graph



is of this type and may be described by the melonic construction

$$(((3), 0, 1), (\underbrace{(2, \dots, 2)}_{n-1}, 1, 1)),$$

where n is the number of circles.

3. Grothendieck classes of melonic graphs

3.1. The Grothendieck ring of varieties

For the category $\mathcal{V}_{\mathbb{K}}$ of varieties over a field \mathbb{K} (which we can here assume to be $\mathbb{K} = \mathbb{Q}$), the Grothendieck group of varieties $K_0(\mathcal{V}_{\mathbb{K}})$ is the abelian group generated by isomorphism classes $[X]$ of varieties $X \in \mathcal{V}_{\mathbb{K}}$ with the inclusion-exclusion relation

$$[X] = [Y] + [X \setminus Y]$$

for closed subvarieties $Y \subset X$. This group may be given a ring structure by defining $[X] \cdot [Y] = [X \times Y]$ and extending by linearity. Grothendieck classes, sometimes referred to as virtual motives, behave like a universal Euler characteristic for algebraic varieties. Grothendieck classes usually provide more computable information about the nature of the motive of a variety. In particular, a Grothendieck class is Tate if it is contained in the subring generated by the Lefschetz motive $\mathbb{L} = [\mathbb{A}^1]$ (the class of an affine line), or equivalently in the ring generated by $\mathbb{T} := \mathbb{L} - 1$. Since the formulas we will obtain will naturally be polynomials in this class, and we will also be interested in expressing them in terms of the class $\mathbb{S} := \mathbb{L} - 2$, we highlight their definitions.

Definition 3.1. We will denote by \mathbb{T} the class of the ‘torus’ in the Grothendieck ring of varieties, i.e., $\mathbb{T} = [\mathbb{A}^1 \setminus \mathbb{A}^0] = \mathbb{L} - 1 \in K_0(\mathcal{V}_{\mathbb{K}})$. We will also denote by \mathbb{S} the class of the complement of three points in \mathbb{P}^1 : $\mathbb{S} = [\mathbb{P}^1 \setminus \{0, 1, \infty\}] = \mathbb{T} - 1$.

Varieties whose motive is in the category of mixed Tate motives will have a Tate Grothendieck class. The converse holds conditionally (see [6] for a discussion of this point).

3.2. Kirchhoff–Symanzik polynomials

We consider the Kirchhoff–Symanzik polynomial of a graph G with n edges

$$\Psi_G(t) = \sum_{T \subset G} \prod_{e \notin E(T)} t_e,$$

as a polynomial in variables $t = (t_1, \dots, t_n)$ associated to the edges of G , with the sum taken over all the spanning trees of the graph. This is a homogeneous polynomial of degree $\ell = b_1(G)$, the first Betti number of the graph, which in physics is referred to as the number of loops of G . Thus, we can consider the associated projective graph hypersurface

$$X_G = \{t = (t_1 : \dots : t_n) \in \mathbb{P}^{n-1} \mid \Psi_G(t) = 0\}.$$

Up to renormalization of divergences, the Feynman parameter form of the Feynman integral for the graph G , for a massless scalar field theory, is of the form

$$U(G, p) = \frac{\Gamma(n - D\ell/2)}{(4\pi)^{\ell D/2}} \int_{\Delta_n} \frac{V_G(t, p)^{-n+\ell D/2}}{\Psi_G(t)^{D/2}} dt_1 \cdots dt_n \quad (3.1)$$

as a function of the external momenta p , where $V_G(t, p)$ is the second Symanzik polynomial (defined in terms of cut sets of G), D is the spacetime dimension, and the integration is performed on the n -simplex. In particular, (modulo divergences) the Feynman integral (3.1) can be regarded as the integration of an algebraic differential form on a locus defined by algebraic equations (that is, a period) on the complement of the hypersurface X_G , hence the interest in investigating the nature of the motive of $\mathbb{P}^{n-1} \setminus X_G$ through the computation of its Grothendieck class. For a general introductory survey of parametric Feynman integrals and their relations to periods and motives of graph hypersurfaces, see [29].

In the following, we will consider both graphs with external edges and graphs (vacuum bubbles) with no external edges. From the point of view of the parametric Feynman integral, the contribution of the external edges with their assigned external momenta is encoded only in the second Symanzik polynomial $V_G(t, p)$, while the variables $t = (t_e)$ run over internal edges. Thus, as long as the exponent satisfies $\ell D/2 \geq n$, with ℓ the number of loops, n the number of (internal) edges, and D the spacetime dimension, the Feynman integral is computed on the complement of the graph hypersurface defined by Kirchhoff–Symanzik polynomial $\Psi_G(t)$ that only depends on the internal edges of G . The Grothendieck class of the affine complement of the hypersurface of a graph G (including external edges) and of the same graph with the external edges removed are simply related by a product by a power of \mathbb{L} (the class of the affine line), hence computing one is equivalent to computing the other. For the purpose of computing Grothendieck classes, considering all graphs (both vacuum bubbles and non-vacuum graphs) for a massless scalar theory with a self-interaction

term of order N , so that the corresponding Feynman graphs have (internal) vertices of valence N , is equivalent to considering all vacuum bubble graphs for a massless scalar theory with self-interaction terms of orders $v \leq N$. For convenience, we will work with graphs with the external edges included.

Up to the issue of renormalization, the Feynman integral (3.1) can then be seen as a period of the graph hypersurface complement. The nature of the motive of the graph hypersurface complement (detected by its Grothendieck class) then provides information on the kind of numbers that can be obtained as periods. The regularization and renormalization of integral (3.1) can also be dealt with geometrically in terms of blowups or deformations. We will not discuss this in the present paper and we refer the reader to [29] for an overview and to the references therein for more information.

3.3. Grothendieck classes of graph hypersurface complements

In previous work, especially [3] and [4], we have focused on the essentially equivalent information given by the complement of the *affine cone* \widehat{X}_G in its ambient affine space, and studied its class in the Grothendieck group of varieties (the ‘motivic Feynman rule’ of [3]). For short, we will refer to this class as the *Grothendieck class* of the graph or of the corresponding melonic construction.

Definition 3.2. The *Grothendieck class* of G (or of any of its melonic constructions) is the class $\mathbb{U}(G) = [\mathbb{A}^n \setminus \widehat{X}_G] \in K_0(\mathcal{V}_{\mathbb{K}})$ of the complement of \widehat{X}_G in its natural ambient affine space \mathbb{A}^n , with n the number of edges of G .

By construction, $\mathbb{U}(G)$ is the class of a variety of dimension equal to the number of edges of G .

In this section, we will use the melonic constructions introduced in Section 2 to obtain a recursive computation of the Grothendieck class of a melonic graph. The class only depends on the isomorphism class of the resulting graph, so equivalent constructions produce the same Grothendieck class.

We recall the following properties of $\mathbb{U}(G)$.

- This invariant is ‘multiplicative’, in the sense that

$$\mathbb{U}(\Gamma_1 \cup \Gamma_2) = \mathbb{U}(\Gamma_1) \cdot \mathbb{U}(\Gamma_2)$$

if Γ_1, Γ_2 are graphs joined at one vertex (or disjoint).

- For $\Gamma =$ a loop, $\mathbb{U}(\Gamma) = \mathbb{T}$ (with \mathbb{T} as in Definition 3.1).
- For $\Gamma =$ a single edge, $\mathbb{U}(\Gamma) = \mathbb{L} = \mathbb{T} + 1$.
- If Γ' is obtained from Γ by splitting an edge, then $\mathbb{U}(\Gamma') = (\mathbb{T} + 1) \cdot \mathbb{U}(\Gamma)$.

- If Γ is an m -banana, $m > 0$, then

$$\mathbb{U}(\Gamma) = \mathbb{B}_m := m\mathbb{T}^{m-1} + \mathbb{T} \cdot \frac{\mathbb{T}^m - (-1)^m}{\mathbb{T} + 1}$$

(see [2] and [4, Corollary 5.6]).

- More generally, if e is not a bridge or a looping edge, then for suitable polynomials f_m, g_m, h_m in \mathbb{T} ,

$$\mathbb{U}(\Gamma_{me}) = f_m \mathbb{U}(\Gamma) + g_m \mathbb{U}(\Gamma/e) + h_m \mathbb{U}(\Gamma \setminus e), \tag{3.2}$$

where

- Γ_{me} stands for the graph obtained from Γ by replacing e with m parallel edges joining the same vertices as e ;
- $\Gamma \setminus e = \Gamma_{0e}$ is Γ with e deleted; and
- Γ/e is Γ with e contracted.

This is a weak form of a deletion-contraction relation. Inductively, the coefficients f_m, g_m, h_m are determined by their value for $m \leq 2$; in fact, we have

$$\begin{aligned} f_m &= \frac{\mathbb{T}^m - (-1)^m}{\mathbb{T} + 1}, \\ g_m &= m\mathbb{T}^{m-1} - \frac{\mathbb{T}^m - (-1)^m}{\mathbb{T} + 1}, \\ h_m &= \frac{\mathbb{T}^m + (-1)^m \mathbb{T}}{\mathbb{T} + 1} \end{aligned} \tag{3.3}$$

as obtained in [4, Corollary 5.7]. Formulas for bridges and looping edges are easier, as they follow immediately from the multiplicativity property.

3.4. Recursion formulas for the Grothendieck classes

The properties listed above, and particularly identity (3.2), lead to recursion formulas for the computation of the Grothendieck class of the melonic graph associated with a melonic construction, or equivalently of the corresponding tree. (We will use the two descriptions interchangeably.) We will abuse language and use both $\mathbb{U}(T)$ and $\mathbb{U}(G)$ for the Grothendieck class of the melonic graph G resulting from a melonic construction T .

The recursion formulas are based on the following observations.

Let G be a melonic graph given by a melonic construction (tree) T .

- By Lemma 2.1, we may assume that the melonic construction is reduced, i.e., nodes labeled 1 are leaves of the tree T .

- If T has length 1, i.e., the corresponding melonic construction consists of a single tuple $((a_1, \dots, a_r), 0, 1)$, then

$$\mathbb{U}(T) = \prod_{i=1}^r \mathbb{B}_{a_i} = \prod_{i=1}^r \left(a_i \mathbb{T}^{a_i-1} + \mathbb{T} \frac{\mathbb{T}^{a_i} - (-1)^{a_i}}{\mathbb{T} + 1} \right).$$

Indeed, the graph G consists of a string of bananas in this case.

If $T = (t_1, \dots, t_n)$ has higher length, consider the last stage t_n . By construction, the black nodes of t_n are all leaves of T .

- If $t_n = ((a), p, k)$, then an equivalent $(n - 1)$ -stage construction is obtained by omitting t_n and increasing the label of the k -th leaf of t_p by $a - 1$.

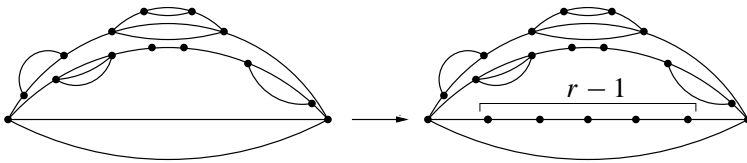


Indeed, this step of the construction simply replaces 1 edge in the k -th banana of t_p by a parallel edges.

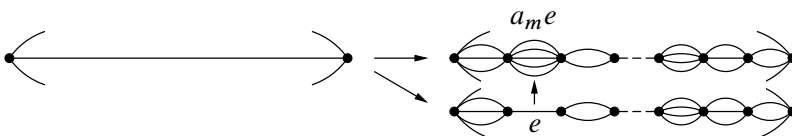
- If

$$t_n = ((\underbrace{1, \dots, 1}_{r \text{ times}}), p, k),$$

then let $T' = (t_1, \dots, t_{n-1})$ be the construction obtained by omitting the last stage. Then $\mathbb{U}(T) = (\mathbb{T} + 1)^{r-1} \mathbb{U}(T')$. Indeed, the effect of t_n is to split one edge in the k -th banana of t_p a total of $r - 1$ times.



- We may therefore assume that $t_n = ((a_1, \dots, a_r), p, k)$ with $r > 1$ and such that $a_m = \max(a_1, \dots, a_r) > 1$. The effect of t_n is to replace one edge in the k -th banana of t_p by a string of $a_1, \dots, a_m, \dots, a_r$ -bananas; this is the same as replacing that edge by a string of $a_1, \dots, a_{m-1}, 1, a_{m+1}, \dots, a_r$ -bananas, and then replacing the resulting single edge e by a_m parallel edges.



Let G' be the graph obtained from G by replacing the a_m -banana by the single edge e . With notation as in (3.2), we have $G = G'_{a_m e}$.

Claim 3.1. *The edge e is not a bridge (or a looping edge) of G' .*

Proof. This follows from the assumption that T is reduced. Indeed, as a consequence the k -th banana of t_p does not consist of a single edge; hence removing one edge of this banana does not disconnect the graph. Since the edge e is one edge in a subdivision of one edge of the k -th banana of t_p , removing it does not disconnect the graph. (And the construction never produces looping edges, therefore e is not a looping edge.) ■

It follows that we can use (3.2) to relate $\mathbb{U}(G)$ to the Grothendieck classes of G' and associated graphs G'/e and $G' \setminus e$

$$\mathbb{U}(G) = f_{a_m} \mathbb{U}(G') + g_{a_m} \mathbb{U}(G'/e) + h_{a_m} \mathbb{U}(G' \setminus e) \tag{3.4}$$

with $f_{a_m}, g_{a_m}, h_{a_m}$ as in (3.3).

Now:

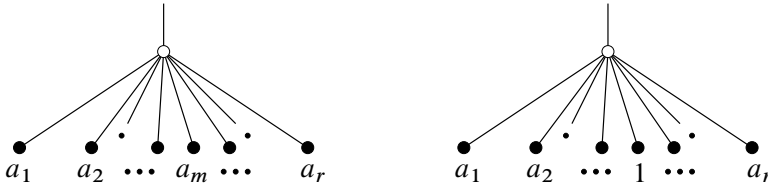
- G' is a melonic graph: its construction T' is obtained from T by replacing

$$t_n = ((a_1, \dots, a_{m-1}, a_m, a_{m+1}, \dots, a_r), p, k)$$

by

$$t'_n = ((a_1, \dots, a_{m-1}, 1, a_{m+1}, \dots, a_r), p, k).$$

Pictorially:



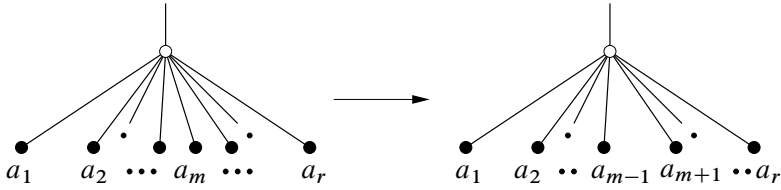
- The contraction G'/e is also a melonic graph: its construction T'' is obtained from T by omitting a_m in t_n , i.e., replacing

$$t_n = ((a_1, \dots, a_{m-1}, a_m, a_{m+1}, \dots, a_r), p, k)$$

by

$$t''_n = ((a_1, \dots, a_{m-1}, a_{m+1}, \dots, a_r), p, k).$$

Since $r > 1$, the tuple $(a_1, \dots, a_{m-1}, a_{m+1}, \dots, a_r)$ is non-empty, as needed (cf. Definition 2.1). Pictorially:



- The deletion $G' \setminus e$ is *not* a melonic graph; it is obtained by replacing one edge of the k -th banana of t_p by two disconnected strings of bananas attached at the vertices of that edge:



Let T''' be the list obtained from T by omitting t_n and decreasing by 1 the order b_k of the k -th banana in t_p . Since T is assumed to be reduced, $b_k > 1$; therefore, T''' is still a melonic construction. (Note that, however, T''' may be *non-reduced*. This is the reason forcing us to consider non-reduced melonic constructions.) The graph $G' \setminus e$ is obtained from the melonic graph corresponding to T''' by attaching two strings of bananas to two vertices, and it follows that

$$\mathbb{U}(G' \setminus e) = \left(\prod_{i=1}^{m-1} \mathbb{B}_{a_i} \right) \left(\prod_{i=m+1}^r \mathbb{B}_{a_i} \right) \mathbb{U}(T''').$$

In conclusion, (3.4) may be rewritten as

$$\mathbb{U}(T) = f_{a_m} \mathbb{U}(T') + g_{a_m} \mathbb{U}(T'') + \left(\prod_{i=1}^{m-1} \mathbb{B}_{a_i} \right) \left(\prod_{i=m+1}^r \mathbb{B}_{a_i} \right) h_{a_m} \mathbb{U}(T'''),$$

or, more explicitly, as follows:

Proposition 3.2. *With notation as above,*

$$\begin{aligned} \mathbb{U}(T) &= \frac{\mathbb{T}^{a_m} - (-1)^{a_m}}{\mathbb{T} + 1} \mathbb{U}(T') + \left(a_m \mathbb{T}^{a_m-1} - \frac{\mathbb{T}^{a_m} - (-1)^{a_m}}{\mathbb{T} + 1} \right) \mathbb{U}(T'') \\ &\quad + \left(\prod_{i=1}^{m-1} \mathbb{B}_{a_i} \right) \left(\prod_{i=m+1}^r \mathbb{B}_{a_i} \right) \frac{\mathbb{T}^{a_m} + (-1)^{a_m} \mathbb{T}}{\mathbb{T} + 1} \mathbb{U}(T'''). \end{aligned}$$

Since T' , T'' , T''' all correspond to melonic graphs with fewer edges than G , the corresponding Grothendieck classes are recursively known, and determine $\mathbb{U}(G) = \mathbb{U}(T)$.

Corollary 3.3. *The graph hypersurface of a melonic graph G determines a mixed Tate motive; the Grothendieck class $\mathbb{U}(G)$ is a polynomial in \mathbb{L} of degree equal to the number of edges of G .*

Proof. The recursion implies immediately that $\mathbb{U}(G)$ is a polynomial in \mathbb{T} , therefore in $\mathbb{L} = \mathbb{T} + 1$. By construction, $\mathbb{U}(G)$ is the class in the Grothendieck group of a variety of dimension equal to the number of edges of G , so the statement follows. ■

3.5. Positivity and log-concavity

The class of a melonic graph can of course also be written as a polynomial in the class $\mathbb{S} = \mathbb{T} - 1 = [\mathbb{P}^1 \setminus \{0, 1, \infty\}]$. Remarkably, these polynomials are ‘positive’, in the following sense.

Corollary 3.4. *Let G be a melonic graph. Then $\mathbb{U}(G) = P(\mathbb{S})$ for a polynomial $P(t) = a_n t^n + \dots + a_1 t + a_0 \in \mathbb{Z}[t]$ with nonnegative integer coefficients.*

Proof. Given the recursion, it suffices to observe that the classes of banana graphs, $\mathbb{B}_m(\mathbb{T}) = \mathbb{B}_m(\mathbb{S} + 1)$, and the coefficients f_m, g_m, h_m are all positive as polynomials in \mathbb{S} . The key observation is the following.

Claim 3.5. *The class*

$$\frac{\mathbb{T}^m - (-1)^m}{\mathbb{T} + 1} = \frac{(\mathbb{S} + 1)^m - (-1)^m}{\mathbb{S} + 2}$$

is positive in \mathbb{S} ; in fact,

$$\frac{\mathbb{T}^m - (-1)^m}{\mathbb{T} + 1} = \sum_{j=1}^{m-1} \sum_{i=1}^{\frac{m}{2}} \binom{m-2i}{j-1} \mathbb{S}^j + \begin{cases} 0 & \text{if } m \text{ is even,} \\ 1 & \text{if } m \text{ is odd.} \end{cases}$$

This is a straightforward computation, left to the reader. Given Claim 3.5, it follows immediately that

$$\mathbb{B}_m = m\mathbb{T}^{m-1} + \mathbb{T} \frac{\mathbb{T}^m - (-1)^m}{\mathbb{T} + 1}, \quad f_m = \frac{\mathbb{T}^m - (-1)^m}{\mathbb{T} + 1}, \quad h_m = \frac{\mathbb{T}^m + (-1)^m \mathbb{T}}{\mathbb{T} + 1}$$

are positive in \mathbb{S} . As for

$$g_m = m\mathbb{T}^{m-1} - \frac{\mathbb{T}^m - (-1)^m}{\mathbb{T} + 1},$$

the required positivity follows from the fact that for all $m, i \geq 1, j$

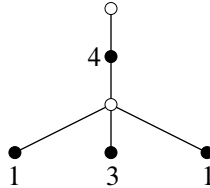
$$\binom{m-1}{j} \geq \binom{m-2i}{j-1}$$

which is clear, as $\binom{m-1}{j} = \binom{m-2}{j-1} + \binom{m-2}{j} \geq \binom{m-2}{j-1} \geq \binom{m-2i}{j-1}$ for $i \geq 1$. ■

Example 3.1. The melon-tadpole graph in Figure 2 consists of a 4-banana tadpole, with class $\mathbb{B}_4 = (\mathbb{T} + 1)(\mathbb{T}^2 + 2\mathbb{T} - 1)\mathbb{T}$, and of a melonic part which may be constructed by

$$(((4), 0, 1), ((1, 3, 1), 1, 1)),$$

i.e., by the labeled tree



The recursion obtained above computes the Grothendieck class of this melonic graph to be

$$\mathbb{T}^2(\mathbb{T} + 1)^4(\mathbb{T}^2 + 3\mathbb{T} - 2).$$

The conclusion is that the Grothendieck class for the graph in Figure 2 equals

$$\begin{aligned} &\mathbb{T}^3(\mathbb{T} + 1)^7(\mathbb{T}^2 + 3\mathbb{T} - 2)(\mathbb{T}^2 + 2\mathbb{T} - 1) \\ &= (\mathbb{S} + 1)^3(\mathbb{S} + 2)^5(\mathbb{S}^2 + 4\mathbb{S} + 2)(\mathbb{S}^2 + 5\mathbb{S} + 2). \end{aligned}$$

Indeed, the graph may be obtained by splitting one edge in each of the two components (which has the effect of multiplying each Grothendieck class by $\mathbb{T} + 1$), and then joining the resulting graphs at the newly created vertices, i.e., multiplying together the two resulting Grothendieck classes. The resulting class is positive in \mathbb{S} .

The positivity of the coefficients of the powers of \mathbb{S} in the Grothendieck class of a melonic graph suggests that these should have a combinatorial interpretation. It would be valuable to have such an interpretation, for example, as a tool to explain the log-concavity property conjectured below. We leave this as an interesting open question. We do not have a compelling answer to this question even in the case of banana graphs.

A Grothendieck class is said to be torified (see [28]) if it may be expressed as a polynomial in \mathbb{T} with nonnegative coefficients. This property may or may not be induced by a geometric torification of the underlying variety. The presence of a torified Grothendieck class has consequences in terms of ‘geometry over the field with one element’ [8, 28]. One can similarly ask whether the positivity of the Grothendieck class as a function of \mathbb{S} is induced by an underlying geometric structure and whether such a structure carries arithmetic significance. For example, the Grothendieck classes of the moduli spaces $\mathcal{M}_{0,n}$ of genus zero curves with marked points have the simple expression

$$[\mathcal{M}_{0,n}] = \binom{\mathbb{S}}{n - 3} (n - 3)!$$

in terms of the class \mathbb{S} , with $[\mathcal{M}_{0,4}] = \mathbb{S}$. However, these classes are not positive in \mathbb{S} , while the classes of the $\bar{\mathcal{M}}_{0,n}$ moduli spaces satisfy positivity (both in \mathbb{S} and in \mathbb{T}), see [28].

Another feature of the polynomials expressing the classes in terms of \mathbb{S} appears to be the following.

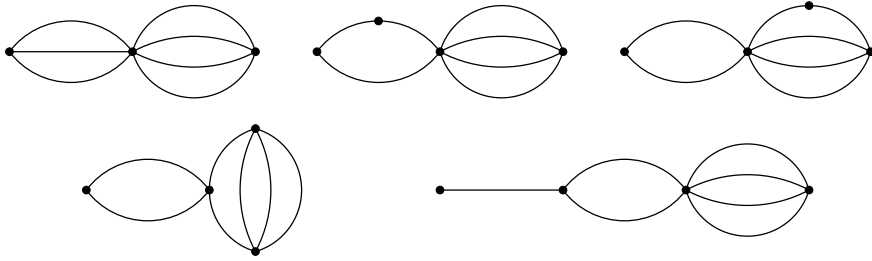
Conjecture 3.1. *Let G be a melonic graph, and let $\mathbb{U}(G) = a_0 + a_1\mathbb{S} + \dots + a_n\mathbb{S}^n$ be its Grothendieck class. Then the sequence a_0, a_1, \dots, a_n is log-concave, i.e., $a_{i-1}a_{i+1} \leq a_i^2$ for $0 < i < n$.*

We have verified this conjecture for all melonic graphs with ≤ 15 edges and for hundreds of individual examples from the families of melonic graphs considered in this paper.

Example 3.2. As polynomials in \mathbb{S} , the Grothendieck classes of all possible melonic graphs with 7 edges are

$$\begin{aligned}
 &(\mathbb{S} + 1)^3(\mathbb{S} + 2)^4, \\
 &(\mathbb{S} + 1)^2(\mathbb{S} + 2)^5, \\
 &(\mathbb{S} + 1)(\mathbb{S} + 2)^6, \\
 &(\mathbb{S} + 2)^7, \\
 &(\mathbb{S} + 1)^3(\mathbb{S} + 2)^3(\mathbb{S} + 3), \\
 &(\mathbb{S} + 1)^2(\mathbb{S} + 2)^4(\mathbb{S} + 3), \\
 &(\mathbb{S} + 1)^3(\mathbb{S} + 2)^3(\mathbb{S} + 4), \\
 &(\mathbb{S} + 1)^4(\mathbb{S} + 2)^2(\mathbb{S} + 5), \\
 &(\mathbb{S} + 1)^2(\mathbb{S} + 2)^3(\mathbb{S}^2 + 4\mathbb{S} + 2), \\
 &(\mathbb{S} + 1)(\mathbb{S} + 2)^4(\mathbb{S}^2 + 4\mathbb{S} + 2), \\
 &(\mathbb{S} + 1)^2(\mathbb{S} + 2)^3(\mathbb{S}^2 + 5\mathbb{S} + 2), \\
 &(\mathbb{S} + 1)^2(\mathbb{S} + 2)^3(\mathbb{S}^2 + 5\mathbb{S} + 5), \\
 &(\mathbb{S} + 1)^2(\mathbb{S} + 2)^2(\mathbb{S}^3 + 6\mathbb{S}^2 + 7\mathbb{S} + 3) \\
 &(\mathbb{S} + 1)(\mathbb{S} + 2)^3(\mathbb{S}^3 + 6\mathbb{S}^2 + 7\mathbb{S} + 3), \\
 &(\mathbb{S} + 1)(\mathbb{S} + 2)^3(\mathbb{S}^3 + 6\mathbb{S}^2 + 9\mathbb{S} + 3), \\
 &(\mathbb{S} + 1)(\mathbb{S} + 2)^2(\mathbb{S}^4 + 8\mathbb{S}^3 + 15\mathbb{S}^2 + 12\mathbb{S} + 3), \\
 &(\mathbb{S} + 1)(\mathbb{S} + 2)^2(\mathbb{S}^4 + 8\mathbb{S}^3 + 19\mathbb{S}^2 + 16\mathbb{S} + 5), \\
 &(\mathbb{S} + 1)(\mathbb{S} + 2)(\mathbb{S}^5 + 10\mathbb{S}^4 + 26\mathbb{S}^3 + 31\mathbb{S}^2 + 17\mathbb{S} + 4).
 \end{aligned}$$

Each of these classes may correspond to several non-isomorphic graphs. For example, note that splitting an edge in two or adding an external edge both have the effect of multiplying the class by $\mathbb{S} + 2$. The graphs



all have Grothendieck class

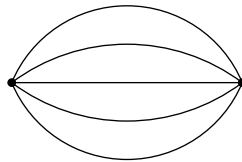
$$(\mathbb{S} + 1)^2(\mathbb{S} + 2)^3(\mathbb{S}^2 + 4\mathbb{S} + 2).$$

One may verify that all these polynomials are log-concave (in the sense that the coefficients of their expansions are log-concave sequences). The number of distinct Grothendieck classes for melonic graphs with n edges is

$$1, 2, 2, 4, 6, 11, 18, 33, 59, 114, 220, 454, 954, 2074, 4602, \dots$$

respectively as $n = 1, 2, 3, \dots$. This list is obtained by direct computation. Melonic (i.e., series-parallel) graphs are enumerated combinatorially in [32].

Remark 3.1. It is well known that if the zeros of a real polynomial are real, then the coefficients of the polynomial form a log-concave sequence (as pointed out in [33], this observation goes back to Newton). The polynomials expressing Grothendieck classes of melonic graphs do not satisfy this stronger condition in general. For example, the polynomial for the 5-banana



is

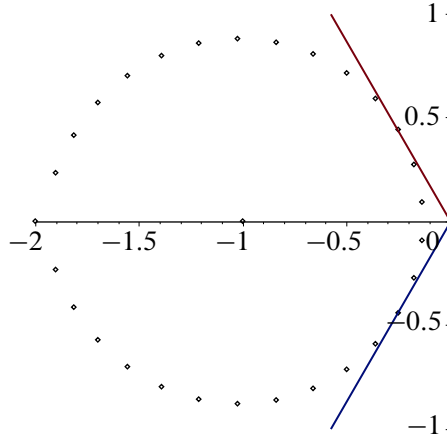
$$(\mathbb{S} + 1)(\mathbb{S} + 2)(\mathbb{S}^3 + 6\mathbb{S}^2 + 7\mathbb{S} + 3)$$

and has two non-real zeros.

In [33] it is also pointed out that a weaker condition on the zeros of a polynomial implies that the coefficients form a log-concave sequence: it suffices that the complex zeros lie in the sector $\{\zeta \mid 2\pi/3 \leq \zeta \leq 4\pi/3\}$ [33, Proposition 7]. This condition is satisfied by the m -banana graph for $m = 1, \dots, 30$, but it fails for $m \geq 31$. The Grothendieck class of the 31-banana is given by

$$m(\mathbb{S} + 1)^{30} + (\mathbb{S} + 1) \cdot \frac{(\mathbb{S} + 1)^{30} - 1}{\mathbb{S} + 2};$$

this polynomial has one real zero close to $\mathbb{S} = -31$, and the others as in the following picture:



Two of the zeros (barely) lie outside the sector.

The necklace graph (as in Remark 2.2) with 24 circles also gives an example.

The log-concavity property of the Grothendieck classes implies similar properties for the images of these classes under any motivic measure, meaning a ring homomorphism $\mu: K_0(\mathcal{V}) \rightarrow R$. Such measures include the topological Euler characteristic and the Hodge–Deligne polynomials (for complex varieties) or the counting of points (for varieties over finite fields). As discussed in [26], the presence of a log-concave structure is usually a sign of the presence of an underlying richer kind of structure, in the form of Hodge–de Rham relations. These can be seen as a broad combinatorial generalization of the setting of the Grothendieck standard conjectures for algebraic cycles. Such combinatorial Hodge–de Rham relations arise, for example, in the context of the log-concavity property of characteristic polynomials of matroids, see [1]. Thus, the observed log-concavity of the Grothendieck classes of the graph hypersurface complements as a polynomial in the \mathbb{S} variable suggests the presence of a more interesting underlying geometric structure in this Hodge–de Rham sense.

While the Grothendieck classes are positive in the class \mathbb{S} and display this intriguing property, we will persist in using \mathbb{T} in most of the examples that follow, since the coefficients of the powers of \mathbb{T} in these classes tend to be smaller and the structure of the resulting expressions is often more transparent. For example, the Grothendieck class of the necklace graph of Remark 2.2, with 10 circles, is

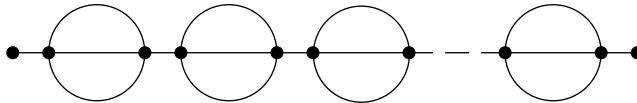
$$\begin{aligned} \mathbb{T}(\mathbb{T} + 1)^9(\mathbb{T}^{10} + 10\mathbb{T}^9 - 1) &= (\mathbb{S} + 1)(\mathbb{S} + 2)^9(\mathbb{S}^{10} + 20\mathbb{S}^9 + 135\mathbb{S}^8 \\ &\quad + 480\mathbb{S}^7 + 1050\mathbb{S}^6 + 1512\mathbb{S}^5 + 1470\mathbb{S}^4 \\ &\quad + 960\mathbb{S}^3 + 405\mathbb{S}^2 + 100\mathbb{S} + 10). \end{aligned}$$

4. Explicit computations, I

The recursion obtained in Section 3 is easily implemented in any symbolic manipulation package, and this makes it possible to explore the landscape of Grothendieck classes for natural families of melonic graphs. We will present a selection of such formulas in the sections that follow. While we are able to prove these formulas (see Section 7), the recursion was key to discovering them, and often the numerical evidence we gathered was quite sufficient to convince us of their truth. It would be worthwhile studying other natural families of melonic graphs using the same method.

In this section, we focus on melonic graph with internal vertices of valence 4, and we will use the shorthand for such graphs introduced in Section 2.

Example 4.1. For a simple valence-4 example that can be computed without employing the full recursion from Section 3, we can consider the graph



with n circles. A corresponding melonic construction is $(0, 1^-, 2^-, 3^-, \dots, (n - 1)^-)$. This construction is non-reduced; a reduced alternative is simply the 1-stage construction

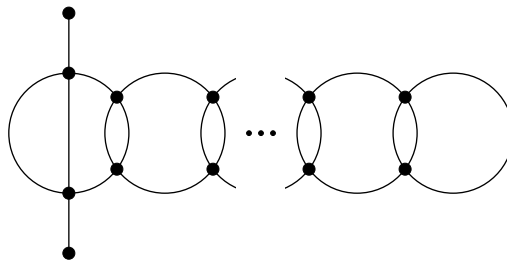
$$((1, 3, 1, 3, 1, 3, \dots, 1), 0, 1).$$

The corresponding Grothendieck class is a product of classes of 3-bananas and $(\mathbb{T} + 1)$ -factors, accounting for the external and internal single edges. Explicitly, the class equals

$$\mathbb{B}_3^n \cdot (\mathbb{T} + 1)^{n+1} = \mathbb{T}^n (\mathbb{T} + 1)^{3n+1}$$

for n circles.

Example 4.2. At the opposite end of the spectrum, and more interestingly, consider the valence-4 melonic graphs Γ_n constructed by $(0, 1^+, 2^+, 3^+, \dots, (n - 1)^+)$. These are graphs of the form



with n circles.

4.1. Recursion for the Γ_n graphs

The graph Γ_n has $4n + 1$ edges, so by Corollary 3.3 its Grothendieck class is a polynomial in \mathbb{T} of degree $4n + 1$. For $n = 1, \dots, 7$, the recursion obtained in Section 3 yields the following Grothendieck classes:

$$\begin{aligned} n = 1: & \quad \mathbb{T}^1(\mathbb{T} + 1)^3 \cdot (\mathbb{T} + 1), \\ n = 2: & \quad \mathbb{T}^2(\mathbb{T} + 1)^5 \cdot (\mathbb{T}^2 + 3\mathbb{T}), \\ n = 3: & \quad \mathbb{T}^3(\mathbb{T} + 1)^7 \cdot (\mathbb{T}^3 + 5\mathbb{T}^2 + 4\mathbb{T} - 2), \\ n = 4: & \quad \mathbb{T}^4(\mathbb{T} + 1)^9 \cdot (\mathbb{T}^4 + 7\mathbb{T}^3 + 12\mathbb{T}^2 - 4), \\ n = 5: & \quad \mathbb{T}^5(\mathbb{T} + 1)^{11} \cdot (\mathbb{T}^5 + 9\mathbb{T}^4 + 24\mathbb{T}^3 + 14\mathbb{T}^2 - 12\mathbb{T} - 4), \\ n = 6: & \quad \mathbb{T}^6(\mathbb{T} + 1)^{13} \cdot (\mathbb{T}^6 + 11\mathbb{T}^5 + 40\mathbb{T}^4 + 48\mathbb{T}^3 - 8\mathbb{T}^2 - 28\mathbb{T}), \\ n = 7: & \quad \mathbb{T}^7(\mathbb{T} + 1)^{15} \cdot (\mathbb{T}^7 + 13\mathbb{T}^6 + 60\mathbb{T}^5 + 110\mathbb{T}^4 + 40\mathbb{T}^3 \\ & \quad - 72\mathbb{T}^2 - 32\mathbb{T} + 8). \end{aligned}$$

The same classes, expressed as polynomials in \mathbb{S} , are

$$\begin{aligned} & (\mathbb{S} + 1)^1(\mathbb{S} + 2)^3(\mathbb{S} + 2), \\ & (\mathbb{S} + 1)^2(\mathbb{S} + 2)^5(\mathbb{S}^2 + 5\mathbb{S} + 4), \\ & (\mathbb{S} + 1)^3(\mathbb{S} + 2)^7(\mathbb{S}^3 + 8\mathbb{S}^2 + 17\mathbb{S} + 8), \\ & (\mathbb{S} + 1)^4(\mathbb{S} + 2)^9(\mathbb{S}^4 + 11\mathbb{S}^3 + 39\mathbb{S}^2 + 49\mathbb{S} + 16), \\ & (\mathbb{S} + 1)^5(\mathbb{S} + 2)^{11}(\mathbb{S}^5 + 14\mathbb{S}^4 + 70\mathbb{S}^3 + 150\mathbb{S}^2 + 129\mathbb{S} + 32), \\ & (\mathbb{S} + 1)^6(\mathbb{S} + 2)^{13}(\mathbb{S}^6 + 17\mathbb{S}^5 + 110\mathbb{S}^4 + 338\mathbb{S}^3 + 501\mathbb{S}^2 + 321\mathbb{S} + 64), \\ & (\mathbb{S} + 1)^7(\mathbb{S} + 2)^{15}(\mathbb{S}^7 + 20\mathbb{S}^6 + 159\mathbb{S}^5 + 640\mathbb{S}^4 + 1375\mathbb{S}^3 + 1524\mathbb{S}^2 \\ & \quad + 769\mathbb{S} + 128). \end{aligned}$$

Identifying the pattern underlying these expressions is an interesting challenge.

- Define polynomials $a_k(r, t) \in \mathbb{Z}[r, t]$ for $k \geq 0$ by the power series expansion

$$e^{rx} \cos((r^2 - rt)^{\frac{1}{2}}x) = \sum_{k \geq 0} a_k(r, t) \frac{x^k}{k!}. \tag{4.1}$$

- In turn, define polynomials $A_n(t) \in \mathbb{Z}[t]$ for $n \geq 0$ by the equality of formal power series

$$\sum_{k \geq 0} a_k(r, t) = \sum_{n \geq 0} A_n(t)r^n.$$

(Since t only appears in the product rt in (4.1), it is clear that $A_n(t)$ is indeed a polynomial, of degree at most n . In fact, $\deg A_n = n$.)

Proposition 4.1. *With Γ_n as above, $\mathbb{U}(\Gamma_n) = \mathbb{T}^n(\mathbb{T} + 1)^{2n+1} \cdot A_n(\mathbb{T})$ for $n \geq 1$.*

Proposition 4.1 may be easily verified for low values of n ; our computer implementation takes a few seconds to verify it for $n = 1, \dots, 100$. We will prove Proposition 4.1 in Section 7.

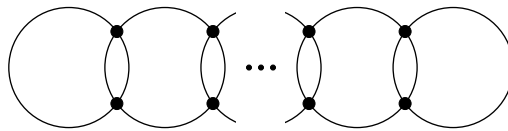
The definition given above for the polynomials $A_n(t)$ is of course just one choice among many. An alternative (and perhaps simpler) formulation will be given in Section 5. The most explicit version of the same result is the following.

Corollary 4.2. *For $n \geq 1$, we have*

$$\begin{aligned} \mathbb{U}(\Gamma_n) &= \mathbb{T}^n(\mathbb{T} + 1)^{2n+1} \cdot \sum_{0 \leq i \leq j} \binom{n+i}{2j} \binom{j}{i} (-1)^{j-i} \mathbb{T}^i \\ &= (\mathbb{S} + 1)^n (\mathbb{S} + 2)^{2n+1} \cdot \sum_{0 \leq i, j} \binom{n-j}{i} \binom{i+j-1}{j} 2^{n-i-j} \mathbb{S}^i. \end{aligned}$$

The straightforward details are left to the reader.

Example 4.3. A similar pattern holds for *vacuum* graphs analogous to those considered in Example 4.2. Let Γ'_n denote the graph



with n circles. As observed at the end of Section 2, these graphs are also melonic: their construction is $((4), 0, 1)$ for two circles and

$$((4), 0, 1), ((1, 3, 1), 1, 1), ((1, 3, 1), 2, 2), \dots, ((1, 3, 1), n - 2, 2)$$

for $n \geq 3$ circles. For $n \geq 2$, Corollary 3.3 implies that $\mathbb{U}(\Gamma'_n)$ is a polynomial of degree $4n - 4$ in \mathbb{T} . Applying the recursion obtained in Section 3, we obtain the following expressions for $\mathbb{U}(\Gamma'_n)$, $n = 2, \dots, 7$:

$$\begin{aligned} n = 2: & \quad \mathbb{T}^1(\mathbb{T} + 1)^1 \cdot (\mathbb{T}^2 + 2\mathbb{T} - 1), \\ n = 3: & \quad \mathbb{T}^2(\mathbb{T} + 1)^3 \cdot (\mathbb{T}^3 + 4\mathbb{T}^2 + \mathbb{T} - 2), \\ n = 4: & \quad \mathbb{T}^3(\mathbb{T} + 1)^5 \cdot (\mathbb{T}^4 + 6\mathbb{T}^3 + 7\mathbb{T}^2 - 4\mathbb{T} - 2), \\ n = 5: & \quad \mathbb{T}^4(\mathbb{T} + 1)^7 \cdot (\mathbb{T}^5 + 8\mathbb{T}^4 + 17\mathbb{T}^3 + 2\mathbb{T}^2 - 12\mathbb{T}), \\ n = 6: & \quad \mathbb{T}^5(\mathbb{T} + 1)^9 \cdot (\mathbb{T}^6 + 10\mathbb{T}^5 + 31\mathbb{T}^4 + 24\mathbb{T}^3 - 22\mathbb{T}^2 - 16\mathbb{T} + 4), \\ n = 7: & \quad \mathbb{T}^6(\mathbb{T} + 1)^{11} \cdot (\mathbb{T}^7 + 12\mathbb{T}^6 + 49\mathbb{T}^5 + 70\mathbb{T}^4 - 8\mathbb{T}^3 - 64\mathbb{T}^2 - 4\mathbb{T} + 8). \end{aligned}$$

As polynomials in \mathbb{S} :

$$\begin{aligned} & (\mathbb{S} + 1)^1(\mathbb{S} + 2)^1 \cdot (\mathbb{S}^2 + 4\mathbb{S} + 2), \\ & (\mathbb{S} + 1)^2(\mathbb{S} + 2)^3 \cdot (\mathbb{S}^3 + 7\mathbb{S}^2 + 12\mathbb{S} + 4), \\ & (\mathbb{S} + 1)^3(\mathbb{S} + 2)^5 \cdot (\mathbb{S}^4 + 10\mathbb{S}^3 + 31\mathbb{S}^2 + 32\mathbb{S} + 8), \\ & (\mathbb{S} + 1)^4(\mathbb{S} + 2)^7 \cdot (\mathbb{S}^5 + 13\mathbb{S}^4 + 59\mathbb{S}^3 + 111\mathbb{S}^2 + 80\mathbb{S} + 16), \\ & (\mathbb{S} + 1)^5(\mathbb{S} + 2)^9 \cdot (\mathbb{S}^6 + 16\mathbb{S}^5 + 96\mathbb{S}^4 + 268\mathbb{S}^3 + 351\mathbb{S}^2 + 192\mathbb{S} + 32), \\ & (\mathbb{S} + 1)^6(\mathbb{S} + 2)^{11} \cdot (\mathbb{S}^7 + 19\mathbb{S}^6 + 142\mathbb{S}^5 + 530\mathbb{S}^4 + 1037\mathbb{S}^3 + 1023\mathbb{S}^2 \\ & \quad + 448\mathbb{S} + 64). \end{aligned}$$

- Define rational functions $a'_k(r, t) \in \mathbb{Z}[t](r)$ for $k \geq 0$ by the power series expansion

$$\cos\left(\frac{(r^2 - rt)^{\frac{1}{2}}}{1 - r}x\right) = \sum_{k \geq 0} a'_k(r, t) \frac{x^k}{k!};$$

that is, let $a'_k(r, t) = 0$ for k odd and $a'_{2\ell}(r, t) = \frac{1}{(2\ell)!} \frac{r^\ell(t-r)^\ell}{(1-r)^{2\ell}}$.

- Define polynomials $A'_n(t) \in \mathbb{Z}[t]$ for $n \geq 0$ by the equality of formal power series

$$\sum_{k \geq 0} a'_k(r, t) = \sum_{n \geq 0} A'_n(t)r^n.$$

(Again, $A'_n(t)$ is clearly a polynomial, and $\deg A'_n = n$.)

Proposition 4.3. *With Γ'_n as above, $\mathbb{U}(\Gamma'_n) = \mathbb{T}^{n-1}(\mathbb{T} + 1)^{2n-3} \cdot A'_n(\mathbb{T})$ for $n \geq 2$.*

Again, Proposition 4.3 may be easily verified by computer, using the recursion formula obtained in Section 3, for (hundreds of) low values of n . Proposition 4.3 will also be proved in Section 7.

Corollary 4.4. *For $n \geq 2$, we have*

$$\begin{aligned} \mathbb{U}(\Gamma'_n) &= \mathbb{T}^{n-1}(\mathbb{T} + 1)^{2n-3} \sum_{0 \leq i \leq j} \binom{n+i-1}{2j-1} \binom{j}{i} (-1)^{j-i} \mathbb{T}^i \\ &= (\mathbb{S} + 1)^{n-1}(\mathbb{S} + 2)^{2n-3} \sum_{0 \leq i \leq j} \binom{n+i-1}{j+i-1} \binom{j}{i} \mathbb{S}^i. \end{aligned}$$

4.2. Relations of vacuum and non-vacuum graphs

A particularly careful reader may notice the following relation from the data shown above:

$$A'_n(t) = A_n(t) - A_{n-1}(t). \tag{4.2}$$

This relation is not a coincidence; it follows from a general formula relating Grothendieck classes of melonic vacuum graphs to classes of related non-vacuum graphs. We will prove this formula in Section 6.

An even more careful reader may guess the divisibility relation

$$\mathbb{U}(\Gamma_n) \mid \mathbb{U}(\Gamma'_{2n+1}), \tag{4.3}$$

for example,

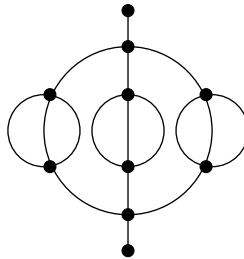
$$A'_7(t) = (t^2 + 5t + 2)(t^2 + 2t - 2) \cdot A_3(t).$$

Relation (4.3) will also be obtained as a corollary of a more general result on melonic vacuum graphs, Proposition 6.3 in Section 6 (see Remark 6.2).

Identity (4.2) can be interpreted within the framework of the operation of *pointing/rooting* in enumerative combinatorics. This in fact corresponds to taking the derivative of the generating function of a class of labelled structures, so that each structure of a certain size n gives rise to n pointed/rooted structures.

More examples of computations of Grothendieck classes for melonic vacuum graphs will be given in Section 6.

The proofs we will discuss in Section 7 will clarify the presence of the factors $\mathbb{T}^i(\mathbb{T} + 1)^j$ in the Grothendieck classes for the valence-4 graphs considered in this section. The example $(0, 1^+, 1^+, 1^+)$



with Grothendieck class

$$\mathbb{T}^3(\mathbb{T} + 1)^{10}(\mathbb{T} + 3)(\mathbb{T}^3 + 3\mathbb{T}^2 - 3\mathbb{T} + 1)$$

shows that $\mathbb{T}^n(\mathbb{T} + 1)^{2n+1}$ is *not* a common factor of the Grothendieck classes of all n -stage valence-4 melonic constructions.

5. Explicit computations, II

5.1. Rational generating functions for Γ_n graphs

While Sections 4 and 6 focus on valence-4 graphs, the same types of computation can be carried out for melonic graphs of any fixed valence for internal vertices. In order

to obtain simpler statements, it is helpful to express the results stated in Examples 4.2 and 4.3 in terms of rational generating functions.

Proposition 5.1. *With notation as in Examples 4.2 and 4.3, and setting $A_0(t) = A'_0(t) = 1$,*

$$\sum_{n \geq 0} A_n(t)r^n = \frac{1-r}{1-(2+t)r+2r^2}, \quad \sum_{n \geq 0} A'_n(t)r^n = \frac{(1-r)^2}{1-(2+t)r+2r^2}.$$

Proof. We verify that the polynomials $A_n(t), A'_n(t)$ defined by these expansions agree with those given in Examples 4.2 and 4.3.

Concerning $A_n(t)$, let $\tau = (r^2 - rt)^{\frac{1}{2}}$; then

$$\frac{1-r}{1-(2+t)r+2r^2} = \frac{1-r}{(1-r-i\tau)(1-r+i\tau)} = \frac{1}{2} \left(\frac{1}{1-r-i\tau} + \frac{1}{1-r+i\tau} \right).$$

The terms in the power series expansion of this expression are combinations of powers of $(r - i\tau)$ and $(r + i\tau)$, so they may be obtained as the coefficients of $\frac{x^k}{k!}$ in

$$\frac{1}{2} (e^{(r+i\tau)x} + e^{(r-i\tau)x}) = e^{rx} \cdot \frac{e^{i\tau x} + e^{-i\tau x}}{2} = e^{rx} \cos(\tau x).$$

This recovers the description of $A_n(t)$ given in Proposition 4.1.

The argument for $A'_n(t)$ is of course analogous. Again setting $\tau = (r^2 - rt)^{\frac{1}{2}}$, we have

$$\begin{aligned} \frac{(1-r)^2}{1-(2+t)r+2r^2} &= \frac{1}{2} \left(\frac{1-r}{1-r-i\tau} + \frac{1-r}{1-r+i\tau} \right) \\ &= \frac{1}{2} \left(\frac{1}{1-i\frac{\tau}{1-r}} + \frac{1}{1+i\frac{\tau}{1-r}} \right) \end{aligned}$$

and the terms in the power series expansion of this expression are the coefficients of $\frac{x^k}{k!}$ in

$$\frac{1}{2} (e^{i\frac{\tau}{1-r}x} + e^{-i\frac{\tau}{1-r}x}) = \cos\left(\frac{\tau}{1-r}x\right),$$

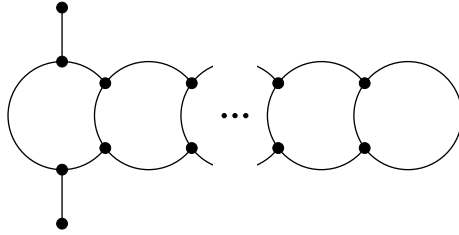
recovering the description of $A'_n(t)$ in Proposition 4.3. ■

5.2. Graphs Γ_n^v with arbitrary valence

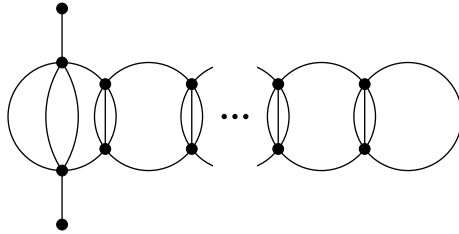
We will discuss some families of valence-4 vacuum graphs in Section 6. The non-vacuum graphs to which the first formula applies have a natural generalization for arbitrary valence: we can let Γ_n^v be the graphs with melonic construction

$$(((1, v-1, 1), 0, 1), ((1, v-1, 1), 1, 2), ((1, v-1, 1), 2, 2), \dots, ((1, v-1, 1), n-1, 2))$$

for $v \geq 3$. For example, the graphs Γ_n^3 have the form



while the graphs Γ_n^5 look like



The first several classes $\mathbb{U}(\Gamma_n^3)$ are

- $n = 1: (\mathbb{T} + 1)^3 \cdot \mathbb{T},$
- $n = 2: (\mathbb{T} + 1)^5 \cdot (\mathbb{T}^2 + \mathbb{T}),$
- $n = 3: (\mathbb{T} + 1)^7 \cdot (\mathbb{T}^3 + 2\mathbb{T}^2),$
- $n = 4: (\mathbb{T} + 1)^9 \cdot (\mathbb{T}^4 + 3\mathbb{T}^3 + \mathbb{T}^2),$
- $n = 5: (\mathbb{T} + 1)^{11} \cdot (\mathbb{T}^5 + 4\mathbb{T}^4 + 3\mathbb{T}^3),$
- $n = 6: (\mathbb{T} + 1)^{13} \cdot (\mathbb{T}^6 + 5\mathbb{T}^5 + 6\mathbb{T}^4 + \mathbb{T}^3),$
- $n = 7: (\mathbb{T} + 1)^{15} \cdot (\mathbb{T}^7 + 6\mathbb{T}^6 + 10\mathbb{T}^5 + 4\mathbb{T}^4).$

It is natural to guess that for $n \geq 1$

$$\mathbb{U}(\Gamma_n^3) = (\mathbb{T} + 1)^{2n+1} \cdot C_n(\mathbb{T})$$

with

$$C_n(\mathbb{T}) = \sum_{i=0}^n \binom{i}{n-i} \mathbb{T}^i. \tag{5.1}$$

This may be proven by induction on the number of circles: the $m = 2$ case of formula (3.2) yields the recursion

$$C_{n+1} = \mathbb{T} \cdot (C_n + C_{n-1}),$$

which determines all C_n from $C_1 = \mathbb{T}, C_2 = \mathbb{T}(\mathbb{T} + 1)$, confirming (5.1). One can package this result as a generating function and draw the following conclusion. Denote by $\langle x^n, F(x) \rangle$ the coefficient of x^n in the series expansion of $F(x)$ at 0.

Proposition 5.2. For $n \geq 1$,

$$\mathbb{U}(\Gamma_n^3) = (\mathbb{T} + 1)^{2n+1} \cdot \left\langle r^n, \frac{1}{1 - \mathbb{T}r - \mathbb{T}r^2} \right\rangle.$$

A similar, but understandably more complex expression holds for arbitrary valence v .

Proposition 5.3. Let $v \geq 4$.

- The class $\mathbb{U}(\Gamma_n^v)$ is a multiple of $\mathbb{T}^n(\mathbb{T} + 1)^{2n+1}$:

$$\mathbb{U}(\Gamma_n^v) = \mathbb{T}^n(\mathbb{T} + 1)^{2n+1} \cdot A_n^v(\mathbb{T})$$

for a polynomial $A_n^v(t)$ of degree $(v - 3)n$.

- The polynomial $A_n^v(t)$ equals the coefficient $\langle r^n, \alpha_v(r, t) \rangle$, where $\alpha_v(r, t)$ is the rational function $N(r, t)/D(r, t)$ with

$$N(r, t) = \frac{1 + t + ((-1)^{v-3} - t^{v-3})r}{1 + t} = 1 - \left(\sum_{i=0}^{v-4} (-1)^{v-i} t^i \right) r$$

and

$$D(r, t) = 1 + \left(-vt^{v-3} - \sum_{i=0}^{v-3} (-1)^{v-i} (i + 2)t^i \right) r + \left((-1)^v t^{v-4} + \sum_{i=0}^{v-4} (-1)^{v-i} (v - 3 - i)t^{v-4+i} \right) r^2.$$

A formal proof of Proposition 5.3 may be constructed along the lines we will provide explicitly for the case $v = 4$ in Section 7.

Example 5.1. Consider the case $v = 10$; the rational function $\alpha_{10}(r, t)$ is

$$\begin{aligned} & (1 - (1 - t + t^2 - t^3 + t^4 - t^5 + t^6)r) \\ & \times (1 - (2 - 3t + 4t^2 - 5t^3 + 6t^4 - 7t^5 + 8t^6 + t^7)r \\ & + (8t^6 - 6t^7 + 5t^8 - 4t^9 + 3t^{10} - 2t^{11} + t^{12})r^2)^{-1} \end{aligned}$$

and the coefficient $\langle r^{13}, \alpha_{10}(r, t) \rangle$ is a polynomial of degree 91:

$$\begin{aligned} & t^{91} + 103t^{90} + 4794t^{89} + \dots - 2455891878317453988t^{45} \\ & + \dots + 866304t^2 - 81920t + 4096. \end{aligned}$$

According to Proposition 5.3, the Grothendieck class for the melonic graph constructed by

$$(((1, 9, 1), 0, 1), ((1, 9, 1), 1, 2), ((1, 9, 1), 2, 2), \dots, ((1, 9, 1), 12, 2))$$

equals

$$\mathbb{T}^{13}(\mathbb{T} + 1)^{27} \cdot (\mathbb{T}^{91} + 103\mathbb{T}^{90} + \dots - 2455891878317453988\mathbb{T}^{45} + \dots - 81920\mathbb{T} + 4096).$$

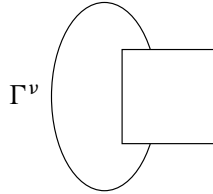
This may be verified by applying the explicit recursion obtained in Section 3.

6. Vacua

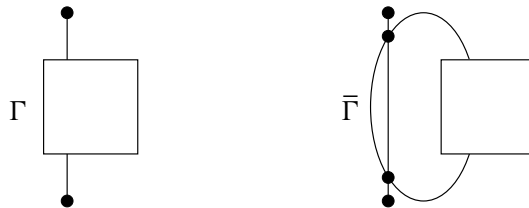
In this section, we focus on melonic vacuum graphs. We first observe that there is a close relation between Grothendieck classes of vacuum graphs and of related *non*-vacuum graphs. For this discussion, the graphs are not necessarily assumed to be melonic; however, the result will explain melonic relations such as the one observed in (4.2).

6.1. Vacuum and non-vacuum graphs relations

Assume that Γ^v is a graph with a distinguished edge



and this edge is not a bridge in Γ^v . Consider two associated graphs: the graph Γ obtained by cutting the edge, and the graph $\bar{\Gamma}$ obtained by inserting a new edge crossing the given edge, with vertices as indicated:



Lemma 6.1. *One has*

$$\mathbb{U}(\Gamma^v) = \frac{\mathbb{U}(\bar{\Gamma}) - \mathbb{T}(\mathbb{T} + 1)^2 \mathbb{U}(\Gamma)}{\mathbb{T}(\mathbb{T} + 1)^4}.$$

Proof. This is an application of the formula for the effect on Grothendieck classes of adding one parallel edge to a given (non-bridge, non-looping) edge in a graph, i.e., the

case $m = 2$ of (3.2). Place two valence-2 vertices on the joined edge in Γ^v , creating an edge e in a graph Γ' ; by construction, e is neither a bridge nor a looping edge. Then

$$\mathbb{U}(\Gamma') = (\mathbb{T} + 1)^2 \mathbb{U}(\Gamma^v), \quad \mathbb{U}(\Gamma'/e) = (\mathbb{T} + 1) \mathbb{U}(\Gamma^v),$$

while $\Gamma' \setminus e = \Gamma$. Replacing e by two parallel edges produces $\bar{\Gamma}$ without the two external edges. Applying (3.2) then gives

$$\frac{\mathbb{U}(\bar{\Gamma})}{(\mathbb{T} + 1)^2} = f_2(\mathbb{T} + 1)^2 \mathbb{U}(\Gamma^v) + g_2(\mathbb{T} + 1) \mathbb{U}(\Gamma^v) + h_2 \mathbb{U}(\Gamma),$$

that is (cf. (3.3))

$$\frac{\mathbb{U}(\bar{\Gamma})}{(\mathbb{T} + 1)^2} = \mathbb{T}(\mathbb{T} + 1)^2 \mathbb{U}(\Gamma^v) + \mathbb{T} \mathbb{U}(\Gamma),$$

with the stated result. ■

In the applications that we have in mind, Γ may be a melonic non-vacuum graph constructed by

$$((1, a_2, \dots, a_{r-1}, 1), 0, 1), t_2, \dots, t_n;$$

the graph Γ^v will then be the (melonic) vacuum graph obtained by joining the two valence-1 vertices of Γ , and $\bar{\Gamma}$ is the non-vacuum graph constructed by

$$((1, 3, 1), 0, 1), ((1, a_2, \dots, a_{r-1}, 1), 1, 2), t'_2, \dots, t'_n,$$

where $t'_i = (b_i, p_i + 1, k_i)$ if $t_i = (b_i, p_i, k_i)$, $i = 2, \dots, n$. Lemma 6.1 shows that the class $\mathbb{U}(\Gamma^v)$ of the vacuum graph is determined by the classes $\mathbb{U}(\Gamma)$, $\mathbb{U}(\bar{\Gamma})$ of the associated non-vacuum graphs.

For example, with notation as in Section 4, Lemma 6.1 implies that

$$\mathbb{U}(\Gamma'_{n+1}) = \frac{\mathbb{U}(\Gamma_{n+1}) - \mathbb{T}(\mathbb{T} + 1)^2 \mathbb{U}(\Gamma_n)}{\mathbb{T}(\mathbb{T} + 1)^4};$$

with $\mathbb{U}(\Gamma_n) = \mathbb{T}^n(\mathbb{T} + 1)^{2n+1} A_n(\mathbb{T})$ and $\mathbb{U}(\Gamma'_n) = \mathbb{T}^{n-1}(\mathbb{T} + 1)^{2n-3} A'_n(\mathbb{T})$ as in Section 4, this relation gives

$$\begin{aligned} & \mathbb{T}^n(\mathbb{T} + 1)^{2n-1} A'_{n+1}(\mathbb{T}) \\ &= \frac{\mathbb{T}^{n+1}(\mathbb{T} + 1)^{2n+3} A_{n+1}(\mathbb{T}) - \mathbb{T}(\mathbb{T} + 1)^2 \mathbb{T}^n(\mathbb{T} + 1)^{2n+1} A_n(\mathbb{T})}{\mathbb{T}(\mathbb{T} + 1)^4}, \end{aligned}$$

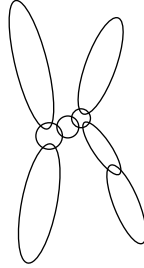
that is,

$$A'_{n+1}(\mathbb{T}) = A_{n+1}(\mathbb{T}) - A_n(\mathbb{T}),$$

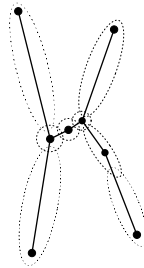
and this proves (4.2).

6.2. Tree structure for valence-four vacua

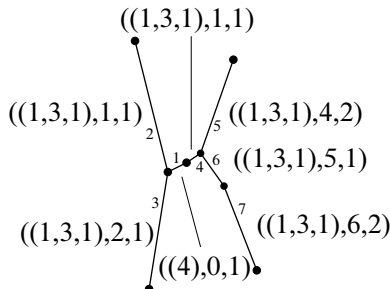
Next, we consider more specifically vacuum bubbles of 2-point melonic graphs in which every vertex has valence 4. These graphs may be drawn as loopless unions of ovals (meaning that the underlying 1-skeleton of the covering by ovals is a tree):



These graphs were discussed in Sections 2.4 and 2.5. The information carried by such a graph is equivalent to the information of a tree, for example, the tree



for the graph shown above. Every node of this tree corresponds to one of the ovals, and two nodes are connected by an edge if and only if the corresponding ovals meet. Given a tree, a corresponding melonic construction is obtained in the evident way by associating one arbitrary edge of the tree with a 4-banana and labeling the other edges with appropriate $((1, 3, 1), *, *)$ tuples as prescribed by adjacencies in the tree. For example, the edges of the above tree could be marked as follows (we also numbered the edges of the tree to reflect the stage of the corresponding tuple in the melonic construction; many other choices are possible):



leading to the melonic construction

$$((4), 0, 1), ((1, 3, 1), 1, 1), ((1, 3, 1), 2, 1), ((1, 3, 1), 1, 1), ((1, 3, 1), 4, 2),$$

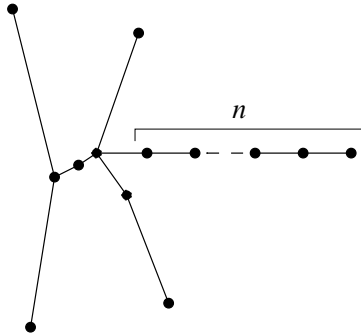
$$((1, 3, 1), 5, 1), ((1, 3, 1), 6, 2). \tag{6.1}$$

Alternatively, one could label one node of the tree by a 2-banana and the remaining nodes by $((1, 3, 1), *, *)$ tuples; the corresponding construction will produce a vacuum melonic graph with two extra valence-2 vertices. This strategy is used below in Example 6.1.

Remark 6.1. Note that a given tree, such as the one shown above, may be used to obtain many different melonic constructions of the same melonic vacuum graph: for example, the root of the melonic construction will depend on which of the edges is (arbitrarily) chosen to carry the initial 4-banana. It would be interesting to obtain a general classification of all melonic constructions giving rise to a given melonic graph, cf. Example 2.3.

6.3. Recursion relations for vacuum bubbles

It is natural to ask whether a simple recursion may exist between the Grothendieck classes of vacuum melonic graphs, reflecting the tree-like structure underlying them. The only instance known to us of such a recursion goes as follows. Assume a branch of the tree projects out of the main body; let U_n denote the Grothendieck class of the vacuum melonic graph obtained by adding n edges to such a branch.

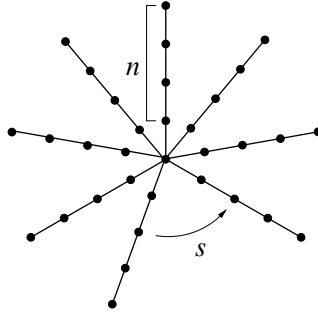


Claim 6.2. For $n \geq 2$,

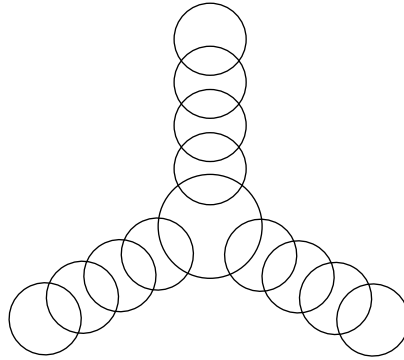
$$U_{n+1} = \mathbb{T}(\mathbb{T} + 1)^2(\mathbb{T} + 2)U_n - 2\mathbb{T}^2(\mathbb{T} + 1)^4U_{n-1}.$$

We will prove this formula in Section 7; in fact, we will prove that this formula holds even if the starting graph is not melonic. This will be our main tool in the proofs of the propositions stated thus far, as well as Proposition 6.3, stated below.

Example 6.1. Let Σ_n^s be the vacuum melonic graph corresponding to the star-shaped tree



with s rays and n nodes along each ray. For example, Σ_4^3 is the following melonic vacuum star:



Interpreting the central node as a 2-banana (thus adding two valence-2 vertices to the corresponding circle) leads to the following melonic construction for Σ_n^s :

$$\begin{aligned}
 &((2), 0, 1), \quad \underbrace{((1, 3, 1, \dots, 3, 1), 1, 1)}_{s \text{ '3' }}, \\
 &((1, 3, 1), 2, 2), \dots, ((1, 3, 1), 2, 2s), \\
 &((1, 3, 1), 3, 2), \dots, ((1, 3, 1), 2 + s, 2), \\
 &((1, 3, 1), 3 + s, 2), \dots, ((1, 3, 1), 2 + 2s, 2), \\
 &\dots, \\
 &((1, 3, 1), 3 + (n - 3)s, 2), \dots, ((1, 3, 1), 2 + (n - 2)s, 2).
 \end{aligned}$$

(Of course, many alternatives are possible.) This construction may be used to compute Grothendieck classes in specific examples, by using the recursion obtained in Section 3 (and dividing by $(\mathbb{T} + 1)^2$ to account for the two additional valence-2 vertices arising in the construction). On the basis of extensive data, one can formulate the following statement.

Proposition 6.3. *Let $\sigma_n^s(t)$ be the polynomials defined by the expansion*

$$\frac{1 - 2r + ((s - 1)t - (s - 2))r^2}{1 - (2 + t)r + 2r^2} = 1 + \sum_{n \geq 0} \sigma_n^s(t)r^{n+1}.$$

Then for $s, n \geq 1$

$$\mathbb{U}(\Sigma_n^s) = \mathbb{T}^{sn}(\mathbb{T} + 1)^{2sn-1} A_n(\mathbb{T})^{s-1} \sigma_n^s(\mathbb{T}),$$

where $A_n(t)$ is the polynomial appearing in Proposition 4.1.

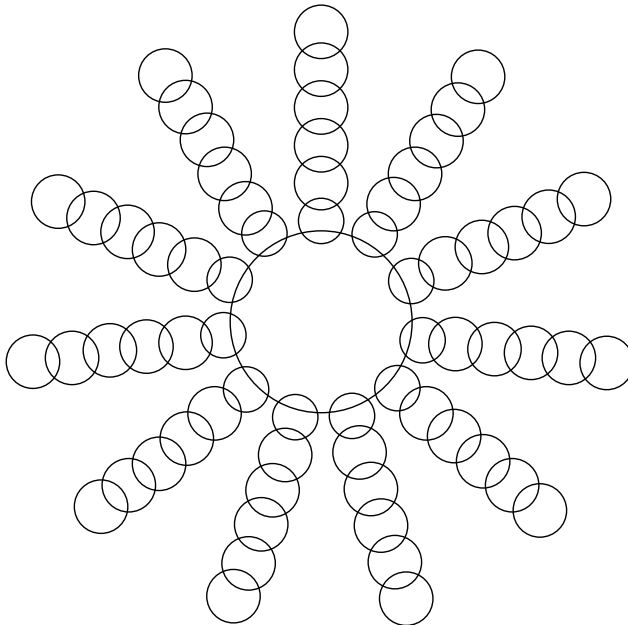
For example, according to the above definition,

$$\sigma_6^{11}(t) = t^7 + 22t^6 + 139t^5 + 290t^4 - 8t^3 - 424t^2 - 44t + 88,$$

and one finds

$$\begin{aligned} \mathbb{T}^{66}(\mathbb{T} + 1)^{131} A_6(\mathbb{T})^{10} \sigma_6^{11}(\mathbb{T}) &= \mathbb{T}^{264} + 263\mathbb{T}^{263} + 34211\mathbb{T}^{262} + 2935019\mathbb{T}^{261} \\ &+ \dots + 26065315469197312\mathbb{T}^{76}, \end{aligned}$$

matching the result of the computation of the Grothendieck class $\mathbb{U}(\Sigma_6^{11})$



by means of the basic recursion obtained in Section 3.

The proof of Proposition 6.3 is given in Section 6. We record the following consequence, which calls for a more geometric explanation. Relation (6.2) below suggests

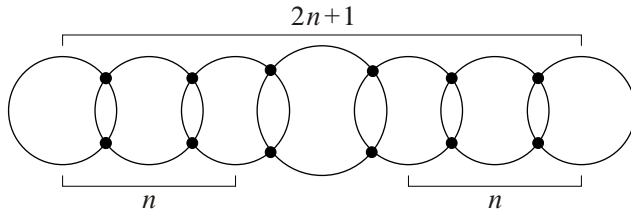
that the complement of the hypersurface $\widehat{X}_{\Sigma_n^s}$ may be realized as a fibration over products of complements of \widehat{X}_{Γ_n} . This suggests the possible presence of interesting geometric relations between these families of graph hypersurfaces.

Corollary 6.4. *If $s \leq 2n$, then $\mathbb{U}(\Gamma_n)^{s-1}$ divides $\mathbb{U}(\Sigma_n^s)$. More precisely,*

$$\mathbb{U}(\Sigma_n^s) = \mathbb{T}^n(\mathbb{T} + 1)^{2n-s} \mathbb{U}(\Gamma_n)^{s-1} \sigma_n^s(\mathbb{T}). \tag{6.2}$$

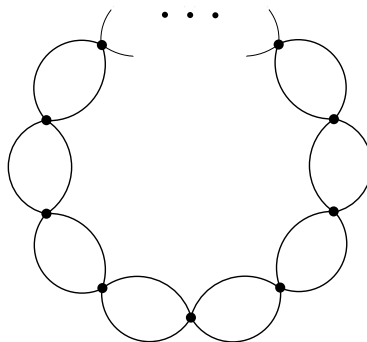
Proof. The given equality follows from the formula given in Proposition 6.3 and the expression for $\mathbb{U}(\Gamma_n)$ obtained in Proposition 4.1. ■

Remark 6.2. Corollary 6.4 implies the divisibility relation (4.3) observed in Section 4. Indeed, the graph Σ_n^2 consists of a string of $2n + 1$ circles:



That is, $\Sigma_n^2 = \Gamma'_{2n+1}$, with notation as in Example 4.3. For this graph, Corollary 6.4 states that $\mathbb{U}(\Gamma_n)$ divides $\mathbb{U}(\Gamma'_{2n+1})$, and this is precisely the assertion in (4.3).

Remark 6.3. Of course, the recursion may be used to compute the Grothendieck class of more general melonic vacuum graphs. For example, the Grothendieck class for the ‘necklace graph’ shown in Remark 2.2,



is

$$(\mathbb{T}^n + n\mathbb{T}^{n-1} - 1)(\mathbb{T} + 1)^{n-1}\mathbb{T},$$

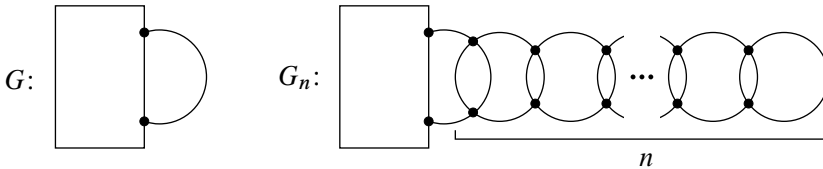
where n is the number of circles. (This may be easily verified by induction.)

7. Proofs

Propositions 4.1 and 4.3 will be proved in the equivalent form presented in Proposition 5.1. For clarity, we will focus on the case of valence 4 given in these propositions; the same method could be used to prove Proposition 5.3.

The statement we will prove will actually be substantially more general than Propositions 4.1 and 4.3: it consists of a recursion ruling the Grothendieck classes of graphs obtained by extending any given graph by a tower of 3-bananas.

Let G be a (not necessarily melonic) graph, and let e be an edge of G . Let G_n be the graph obtained by applying a chain of $(1, 3, 1)$ -bananifications starting from e :

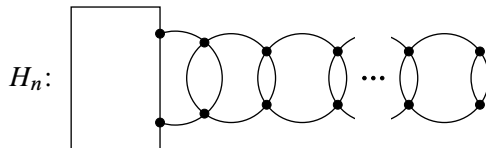


Theorem 7.1. *The generating function for the Grothendieck classes $\mathbb{U}(G_n)$ is rational, with denominator independent of G . More precisely, there exists a polynomial $P(\mathbb{T}, \rho)$ with integer coefficients such that*

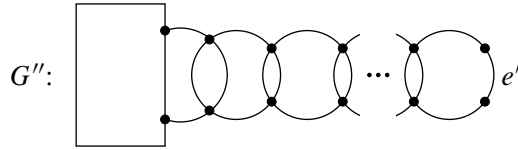
$$\sum_{n \geq 0} \mathbb{U}(G_n) \rho^n = \frac{P(\mathbb{T}, \rho)}{1 - \mathbb{T}(\mathbb{T} + 1)^2(\mathbb{T} + 2)\rho + 2\mathbb{T}^2(\mathbb{T} + 1)^4 \rho^2}.$$

This statement focuses on the fact that the generating function is rational and gives an explicit form for its denominator, which depends on the bananification process itself rather than on the graph G . The graph G determines the numerator $P(\mathbb{T}, \rho)$; explicit formulas will be given below in Theorem 7.2. For example, we will see that the polynomial has degree 1 in ρ , and $P(\mathbb{T}, 0) = \mathbb{U}(G)$.

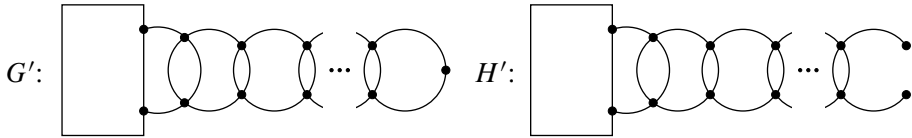
Proof. Denote by H_n the graph obtained from G_n by replacing the last 3-bananification with a 2-bananification:



Denote $\mathbb{U}(G_n)$ by U_n , $\mathbb{U}(H_n)$ by V_n . Assume $n \geq 2$. Consider the graph G'' obtained by splitting one of the parallel edges of the top banana in G_{n-1} into three edges; let e' be the central edge so produced, and note that e' is not a bridge or a looping edge of G'' .



The contraction $G' := G''/e'$ may be obtained from G_{n-1} by splitting the same edge of the top banana into *two* edges, and the deletion $H' = G'' \setminus e'$ may be obtained from H_{n-1} by attaching two external edges to the vertices of the top (2-)banana:



By (3.2), we have

$$\begin{aligned} V_n &= f_2 \mathbb{U}(G'') + g_2 \mathbb{U}(G') + h_2 \mathbb{U}(H'), \\ U_n &= f_3 \mathbb{U}(G'') + g_3 \mathbb{U}(G') + h_3 \mathbb{U}(H'), \end{aligned}$$

where f_2, f_3 , etc., are as in (3.3). We now note that

$$\begin{cases} \mathbb{U}(G'') = (\mathbb{T} + 1)^2 \mathbb{U}(G_{n-1}) = (\mathbb{T} + 1)^2 U_{n-1}, \\ \mathbb{U}(G') = (\mathbb{T} + 1) \mathbb{U}(G_{n-1}) = (\mathbb{T} + 1) U_{n-1}, \\ \mathbb{U}(H') = (\mathbb{T} + 1)^2 \mathbb{U}(H_{n-1}) = (\mathbb{T} + 1)^2 V_{n-1}, \end{cases}$$

further,

$$\begin{aligned} f_2(\mathbb{T} + 1)^2 + g_2(\mathbb{T} + 1) &= \mathbb{T}(\mathbb{T} + 1)^2, \\ f_3(\mathbb{T} + 1)^2 + g_3(\mathbb{T} + 1) &= \mathbb{T}(\mathbb{T} + 1)^3, \end{aligned}$$

while $h_2 = \mathbb{T}, h_3 = (\mathbb{T} - 1)\mathbb{T}$. The above formulas can then be rewritten as

$$\begin{aligned} V_n &= \mathbb{T}(\mathbb{T} + 1)^2 U_{n-1} + \mathbb{T}(\mathbb{T} + 1)^2 V_{n-1}, \\ U_n &= \mathbb{T}(\mathbb{T} + 1)^3 U_{n-1} + (\mathbb{T} - 1)\mathbb{T}(\mathbb{T} + 1)^2 V_{n-1}. \end{aligned} \tag{7.1}$$

These imply

$$\begin{aligned} (\mathbb{T} - 1)V_n &= (\mathbb{T} - 1)\mathbb{T}(\mathbb{T} + 1)^2 U_{n-1} + (\mathbb{T} - 1)\mathbb{T}(\mathbb{T} + 1)^2 V_{n-1} \\ &= (\mathbb{T} - 1)\mathbb{T}(\mathbb{T} + 1)^2 U_{n-1} + (U_n - \mathbb{T}(\mathbb{T} + 1)^3 U_{n-1}) \\ &= U_n - 2\mathbb{T}(\mathbb{T} + 1)^2 U_{n-1} \end{aligned}$$

and therefore

$$\begin{aligned} U_{n+1} &= \mathbb{T}(\mathbb{T} + 1)^3 U_n + (\mathbb{T} - 1)\mathbb{T}(\mathbb{T} + 1)^2 V_n \\ &= \mathbb{T}(\mathbb{T} + 1)^3 U_n + \mathbb{T}(\mathbb{T} + 1)^2 (U_n - 2\mathbb{T}(\mathbb{T} + 1)^2 U_{n-1}) \\ &= \mathbb{T}(\mathbb{T} + 1)^2 (\mathbb{T} + 2) U_n - 2\mathbb{T}^2 (\mathbb{T} + 1)^4 U_{n-1}. \end{aligned}$$

(This proves Claim 6.2.) Now, for $n \geq 2$, the coefficient of ρ^{n+1} in the product

$$(1 - \mathbb{T}(\mathbb{T} + 1)^2 (\mathbb{T} + 2)\rho + 2\mathbb{T}^2 (\mathbb{T} + 1)^4 \rho^2) \cdot \sum_{n \geq 0} U_n \rho^n$$

equals

$$U_{n+1} - \mathbb{T}(\mathbb{T} + 1)^2 (\mathbb{T} + 2) U_n + 2\mathbb{T}^2 (\mathbb{T} + 1)^4 U_{n-1} = 0.$$

This product is therefore a polynomial $P(\mathbb{T}, \rho)$, and this proves the statement. ■

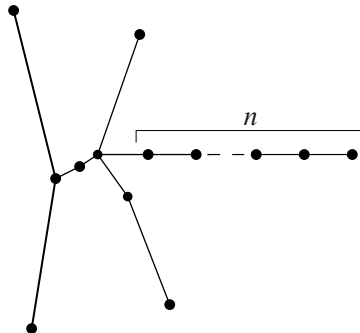
The argument shows that

$$\begin{aligned} P(\mathbb{T}, \rho) &= (1 - \mathbb{T}(\mathbb{T} + 1)^2 (\mathbb{T} + 2)\rho + 2\mathbb{T}^2 (\mathbb{T} + 1)^4 \rho^2) \cdot \sum_{n \geq 0} U_n \rho^n \\ &= \mathbb{U}(G) + (\mathbb{U}(G_1) - \mathbb{T}(\mathbb{T} + 1)^2 (\mathbb{T} + 2)\mathbb{U}(G))\rho \\ &\quad + (\mathbb{U}(G_2) - \mathbb{T}(\mathbb{T} + 1)^2 (\mathbb{T} + 2)\mathbb{U}(G_1) \\ &\quad + 2\mathbb{T}^2 (\mathbb{T} + 1)^4 \mathbb{U}(G))\rho^2. \end{aligned} \tag{7.2}$$

If e is not a bridge, then the argument proves the same recursion for $n \geq 1$; it follows that the coefficient $\langle \rho^2, P(\mathbb{T}, \rho) \rangle$ of ρ^2 in $P(\mathbb{T}, \rho)$ is 0 in this case. Maybe a little surprisingly, the same conclusion holds if e is a bridge (as we will prove below); thus, the polynomial $P(\mathbb{T}, \rho)$ is of degree 1 in ρ . This polynomial is determined by $\mathbb{U}(G)$ and the deletion $\mathbb{U}(G \setminus e)$, as we will see below.

In fact, Theorem 7.1 and the direct computation of a few values of $\mathbb{U}(G_n)$ suffice to determine the numerator.

Example 7.1. The melonic valence-4 vacuum graphs corresponding to the trees



have melonic construction obtained by extending (6.1):

$$\begin{aligned} &((4), 0, 1), ((1, 3, 1), 1, 1), ((1, 3, 1), 2, 1), ((1, 3, 1), 1, 1), ((1, 3, 1), 4, 2), \\ &((1, 3, 1), 5, 1), ((1, 3, 1), 6, 2), ((1, 3, 1), 6, 1), ((1, 3, 1), 8, 2), \dots, \\ &((1, 3, 1), n + 6, 2). \end{aligned}$$

Using the recursion obtained in Section 3, we can compute the following Grothendieck classes:

$$\begin{aligned} n = 0: & \mathbb{T}^7(\mathbb{T} + 1)^{14}(\mathbb{T}^7 + 13\mathbb{T}^6 + 56\mathbb{T}^5 + 80\mathbb{T}^4 - 17\mathbb{T}^3 - 77\mathbb{T}^2 + 8), \\ n = 1: & \mathbb{T}^8(\mathbb{T} + 1)^{17}(\mathbb{T}^7 + 14\mathbb{T}^6 + 64\mathbb{T}^5 + 94\mathbb{T}^4 - 29\mathbb{T}^3 - 100\mathbb{T}^2 + 12\mathbb{T} + 8), \\ n = 2: & \mathbb{T}^{10}(\mathbb{T} + 1)^{18}(\mathbb{T} + 3)(\mathbb{T}^7 + 14\mathbb{T}^6 + 64\mathbb{T}^5 + 96\mathbb{T}^4 - 19\mathbb{T}^3 \\ & \quad - 102\mathbb{T}^2 - 6\mathbb{T} + 16) \end{aligned}$$

and this is (more than) enough information to determine $P(\mathbb{T}, \rho)$: if U_0, U_1, U_2 are these three classes, the product

$$(1 - \mathbb{T}(\mathbb{T} + 1)^2(\mathbb{T} + 2)\rho + 2\mathbb{T}^2(\mathbb{T} + 1)^4\rho^2) \cdot (U_0 + U_1\rho + U_2\rho^2)$$

equals

$$\begin{aligned} &\mathbb{T}^7(\mathbb{T} + 1)^{14}(\mathbb{T}^7 + 13\mathbb{T}^6 + 56\mathbb{T}^5 + 80\mathbb{T}^4 - 17\mathbb{T}^3 - 77\mathbb{T}^2 + 8) \\ &\quad - 2\mathbb{T}^8(\mathbb{T} + 1)^{16}(2\mathbb{T}^6 + 17\mathbb{T}^5 + 39\mathbb{T}^4 + 9\mathbb{T}^3 - 33\mathbb{T}^2 - 6\mathbb{T} + 4)\rho \end{aligned}$$

modulo ρ^3 . As expected, the coefficient of ρ^2 vanishes. The polynomial $P(\mathbb{T}, \rho)$ must equal this degree 1 polynomial in ρ .

In general, $P(\mathbb{T}, \rho)$ is determined by the Grothendieck classes of G and (if e is not a bridge) $G \setminus e$, if the latter is known.

Theorem 7.2. *With notation as above, let $r = \mathbb{T}(\mathbb{T} + 1)^2\rho$. Then we have*

$$\sum_{n \geq 0} \mathbb{U}(G_n)\rho^n = \frac{1 - r}{1 - (\mathbb{T} + 2)r + 2r^2} \cdot \mathbb{U}(G)$$

if e is a bridge in G , and

$$\sum_{n \geq 0} \mathbb{U}(G_n)\rho^n = \frac{\mathbb{U}(G) + ((\mathbb{T} - 1)\mathbb{U}(G \setminus e) - \mathbb{U}(G))r}{1 - (\mathbb{T} + 2)r + 2r^2}$$

if e is not a bridge in G .

Proof. The argument proving Theorem 7.1 shows that $\langle \rho^n, P(\mathbb{T}, \rho) \rangle = 0$ for $n \geq 3$, and for $n \geq 2$ if e is not a bridge, as observed above. If e is a bridge,

$$U_1 = (T + 1)^2 \mathbb{B}(3) \mathbb{U}(G \setminus e) = \mathbb{T}(\mathbb{T} + 1)^4 \mathbb{U}(G \setminus e) = \mathbb{T}(\mathbb{T} + 1)^3 U_0,$$

since G_1 is obtained by replacing the central split of e , a bridge, with a 3-banana. By the same token,

$$V_1 = (T + 1)^2 \mathbb{B}(2) \mathbb{U}(G \setminus e) = \mathbb{T}(\mathbb{T} + 1)^3 \mathbb{U}(G \setminus e) = \mathbb{T}(\mathbb{T} + 1)^2 U_0.$$

By (7.1), we have

$$U_2 = \mathbb{T}(\mathbb{T} + 1)^3 U_1 + (\mathbb{T} - 1) \mathbb{T}(\mathbb{T} + 1)^2 V_1 = \mathbb{T}^3 (\mathbb{T} + 1)^4 (\mathbb{T} + 3) U_0.$$

On the other hand,

$$\begin{aligned} & \mathbb{T}(\mathbb{T} + 1)^2 (\mathbb{T} + 2) U_1 - 2 \mathbb{T}^2 (\mathbb{T} + 1)^4 U_0 \\ &= \mathbb{T}^2 (\mathbb{T} + 1)^5 (\mathbb{T} + 2) U_0 - 2 \mathbb{T}^2 (\mathbb{T} + 1)^4 U_0 = \mathbb{T}^3 (\mathbb{T} + 1)^4 (\mathbb{T} + 3) U_0. \end{aligned}$$

This verifies that $\langle \rho^2, P(\mathbb{T}, \rho) \rangle = 0$ in this case as well (see (7.2)). Therefore, in all cases we have

$$P(\mathbb{T}, \rho) = \mathbb{U}(G) + (\mathbb{U}(G_1) - \mathbb{T}(\mathbb{T} + 1)^2 (\mathbb{T} + 2) \mathbb{U}(G)) \rho.$$

If e is a bridge,

$$\langle \rho, P(\mathbb{T}, \rho) \rangle = \mathbb{U}(G_1) - \mathbb{T}(\mathbb{T} + 1)^2 (\mathbb{T} + 2) \mathbb{U}(G) = -\mathbb{T}(\mathbb{T} + 1)^2 \mathbb{U}(G)$$

since $\mathbb{U}(G_1) = U_1 = \mathbb{T}(\mathbb{T} + 1)^3 U_0 = \mathbb{T}(\mathbb{T} + 1)^3 \mathbb{U}(G)$ as we observed above. Therefore,

$$P(\mathbb{T}, \rho) = \mathbb{U}(G) - \mathbb{T}(\mathbb{T} + 1)^2 \mathbb{U}(G) \rho = (1 - r) \mathbb{U}(G)$$

if e is a bridge, and this gives the first formula.

If e is not a bridge, splitting it into three and 3-bananifying the central edge gives, arguing as in the proof of Theorem 7.1,

$$\mathbb{U}(G_1) = \mathbb{T}(\mathbb{T} + 1)^3 \mathbb{U}(G) + (\mathbb{T} - 1) \mathbb{T}(\mathbb{T} + 1)^2 \mathbb{U}(G \setminus e)$$

and therefore

$$\begin{aligned} & \mathbb{U}(G_1) - \mathbb{T}(\mathbb{T} + 1)^2 (\mathbb{T} + 2) \mathbb{U}(G) \\ &= -\mathbb{T}(\mathbb{T} + 1)^2 \mathbb{U}(G) + (\mathbb{T} - 1) \mathbb{T}(\mathbb{T} + 1)^2 \mathbb{U}(G \setminus e). \end{aligned}$$

It follows that the degree-1 term in $P(\mathbb{T}, \rho)$ in this case is

$$(-\mathbb{U}(G) + (\mathbb{T} - 1) \mathbb{U}(G \setminus e)) \mathbb{T}(\mathbb{T} + 1)^2 \rho,$$

and this completes the proof of the second formula. ■

The fact that the formulas in Theorem 7.2 depend on $r = \mathbb{T}(\mathbb{T} + 1)^2\rho$ explains why the specific examples worked out in Propositions 4.1 and 4.3 included powers of \mathbb{T} and $\mathbb{T} + 1$ as stated. We recover these results in the next two examples.

Example 7.2. Define the polynomials $A_n(t)$ by the power series expansion

$$\sum_{n \geq 0} A_n(t)r^n = \frac{1 - r}{1 - (2 + t)r + 2r^2}$$

(cf. Proposition 5.1). Then the first formula in Theorem 7.2 reads

$$\sum_{n \geq 0} \mathbb{U}(G_n)\rho^n = \left(\sum_{n \geq 0} A_n(t)r^n \right) \cdot \mathbb{U}(G) = \left(\sum_{n \geq 0} A_n(\mathbb{T})\mathbb{T}^n(\mathbb{T} + 1)^{2n}\rho^n \right) \cdot \mathbb{U}(G).$$

Equivalently,

$$\mathbb{U}(G_n) = \mathbb{T}^n(\mathbb{T} + 1)^{2n}A_n(\mathbb{T}) \cdot \mathbb{U}(G). \tag{7.3}$$

If G consists of a single edge, then with notation as in Section 4 we have $G_n = \Gamma_n$, and $\mathbb{U}(G) = \mathbb{T} + 1$, therefore (7.3) gives

$$\mathbb{U}(\Gamma_n) = \mathbb{T}^n(\mathbb{T} + 1)^{2n+1}A_n(\mathbb{T}),$$

proving Proposition 4.1 (in the form given in Proposition 5.1).

Example 7.3. Now let G be a 2-banana, and let e be one of its (two) edges. The graph $G \setminus e$ is a single edge. Therefore,

$$\mathbb{U}(G) = \mathbb{T}(\mathbb{T} + 1), \quad \mathbb{U}(G \setminus e) = \mathbb{T} + 1,$$

and the second formula in Theorem 7.2 states that

$$\begin{aligned} \sum_{n \neq 0} \mathbb{U}(G_n)\rho^n &= \frac{\mathbb{T}(\mathbb{T} + 1) + ((\mathbb{T} - 1)(\mathbb{T} + 1) - \mathbb{T}(\mathbb{T} + 1))r}{1 - (\mathbb{T} + 2)r + 2r^2} \\ &= \frac{\mathbb{T} - r}{1 - (\mathbb{T} + 2)r + 2r^2} \cdot (\mathbb{T} + 1). \end{aligned}$$

With notation as in Section 4, the graph G_n (consisting of a chain of $n + 1$ circles) equals Γ'_{n+1} , with two extra valence-2 vertices on the first circle. That is,

$$\mathbb{U}(\Gamma'_n) = \frac{\mathbb{U}(G_{n-1})}{(\mathbb{T} + 1)^2}.$$

Now, since $r = \mathbb{T}(\mathbb{T} + 1)^2\rho$, the coefficient of ρ^{n-1} may be expressed in terms of the coefficient of r^{n-1} :

$$\mathbb{U}(G_{n-1}) = \mathbb{T}^{n-1}(\mathbb{T} + 1)^{2n-2} \left\langle r^{n-1}, \frac{(\mathbb{T} - r)(\mathbb{T} + 1)}{1 - (\mathbb{T} + 2)r + 2r^2} \right\rangle$$

hence

$$\frac{\mathbb{U}(G_{n-1})}{(\mathbb{T} + 1)^2} = \mathbb{T}^{n-1}(\mathbb{T} + 1)^{2n-3} \left\langle r^{n-1}, \frac{(\mathbb{T} - r)}{1 - (\mathbb{T} + 2)r + 2r^2} \right\rangle$$

and therefore

$$\mathbb{U}(\Gamma'_n) = \mathbb{T}^{n-1}(\mathbb{T} + 1)^{2n-3} \left\langle r^n, \frac{r(\mathbb{T} - r)}{1 - (\mathbb{T} + 2)r + 2r^2} \right\rangle.$$

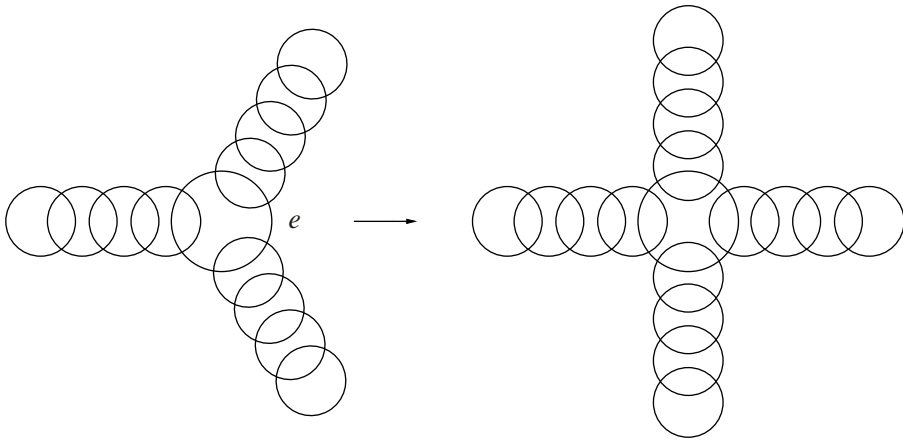
This holds for $n \geq 1$; setting (as in Section 4) the constant term of the relevant series to 1 amounts to adding 1 to this rational function, and we have

$$1 + \frac{r(\mathbb{T} - r)}{1 - (\mathbb{T} + 2)r + 2r^2} = \frac{(1 - r)^2}{1 - (\mathbb{T} + 2)r + 2r^2}$$

verifying Proposition 4.3, in the form given in Proposition 5.1.

Example 7.4. As a final example, we will prove Proposition 6.3, by induction on the number s of rays. For $s = 1$, the statement reproduces Proposition 4.3; so we only need to prove the induction step, and we may assume $s > 1$.

To transition from Σ_n^{s-1} to Σ_n^s , view Σ_n^s as the graph obtained by adding a chain of 3-bananas to one of the edges e of the central circle in $G = \Sigma_n^{s-1}$.



Since e is not a bridge, we can apply the second formula given in Theorem 7.2. We write it as follows:

$$\frac{1 - r}{1 - (\mathbb{T} + 2)r + 2r^2} \mathbb{U}(\Sigma_n^{s-1}) + \frac{r(\mathbb{T} - 1)}{1 - (\mathbb{T} + 2)r + 2r^2} \mathbb{U}(\Sigma_n^{s-1} \setminus e).$$

The class $\mathbb{U}(\Sigma_n^s)$ is the coefficient of ρ^n in this expression (i.e., $\mathbb{T}^n(\mathbb{T} + 1)^{2n}$ times the coefficient of r^n). We will deal with the two summands separately.

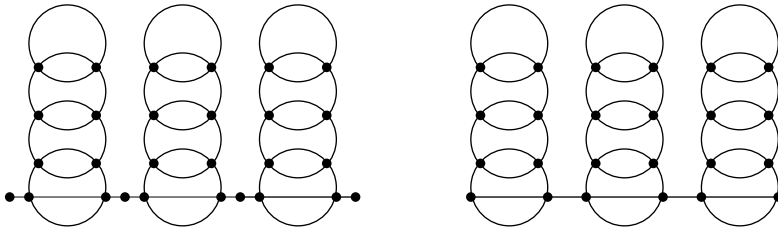
- By induction on s , the coefficient in the first summand equals

$$\frac{\mathbb{U}(\Gamma_n)}{(\mathbb{T} + 1)} \cdot \mathbb{T}^{(s-1)n} (\mathbb{T} + 1)^{2(s-1)n-1} A_n(\mathbb{T})^{s-2} \times \left\langle r^{n+1}, \frac{1 - 2r + ((s-2)\mathbb{T} - (s-3))r^2}{1 - (\mathbb{T} + 2)r + 2r^2} \right\rangle$$

and $\mathbb{U}(\Gamma_n) = \mathbb{T}^n (\mathbb{T} + 1)^{2n+1} A_n(\mathbb{T})$, so this equals

$$\mathbb{T}^{sn} (\mathbb{T} + 1)^{2sn-1} A_n(\mathbb{T})^{s-1} \left\langle r^{n+1}, \frac{1 - 2r + ((s-2)\mathbb{T} - (s-3))r^2}{1 - (\mathbb{T} + 2)r + 2r^2} \right\rangle.$$

- In the second summand, $\Sigma_n^{s-1} \setminus e$ consists of a join of $s - 1$ chains of n -circles, therefore its Grothendieck class $\mathbb{U}(\Sigma_n^{s-1} \setminus e)$ is the $(s - 1)$ -st power of $\mathbb{U}(\Gamma_n)$, up to an appropriate factor of $(\mathbb{T} + 1)$ to account for the fact that $\Sigma_n^{s-1} \setminus e$ has no valence-2 vertices and no external edges. For example, here is a picture contrasting the join of 3 graphs Γ_4 (on the left) with $\Sigma_4^3 \setminus e$ (on the right):



It follows that

$$\mathbb{U}(\Sigma_n^{s-1} \setminus e) = \frac{\mathbb{U}(\Gamma_n)^{s-1}}{(\mathbb{T} + 1)^s} = \mathbb{T}^{(s-1)n} (\mathbb{T} + 1)^{2(s-1)n-1} A_n(\mathbb{T})^{s-1}.$$

Therefore, the coefficient in the second summand equals

$$\mathbb{T}^{(s-1)n} (\mathbb{T} + 1)^{2(s-1)n-1} A_n(\mathbb{T})^{s-1} \left\langle \rho^n, \frac{r(\mathbb{T} - 1)}{1 - (\mathbb{T} + 2)r + 2r^2} \right\rangle.$$

Now, the coefficient of ρ^n equals $\mathbb{T}(\mathbb{T} + 1)^2$ times the coefficient of r^n , so this may be rewritten as

$$\mathbb{T}^{sn} (\mathbb{T} + 1)^{2sn-1} A_n(\mathbb{T})^{s-1} \left\langle r^n, \frac{r(\mathbb{T} - 1)}{1 - (\mathbb{T} + 2)r + 2r^2} \right\rangle$$

or equivalently

$$\mathbb{T}^{sn} (\mathbb{T} + 1)^{2sn-1} A_n(\mathbb{T})^{s-1} \left\langle r^{n+1}, \frac{r^2(\mathbb{T} - 1)}{1 - (\mathbb{T} + 2)r + 2r^2} \right\rangle.$$

Putting the summands back together, we see that $\mathbb{U}(\Sigma_n^s)$ equals $\mathbb{T}^{sn}(\mathbb{T} + 1)^{2sn-1} \times A_n(\mathbb{T})^{s-1}$ times the coefficient of r^{n+1} in

$$\begin{aligned} & \frac{1 - 2r + ((s - 2)\mathbb{T} - (s - 3))r^2}{1 - (\mathbb{T} + 2)r + 2r^2} + \frac{r^2(\mathbb{T} - 1)}{1 - (\mathbb{T} + 2)r + 2r^2} \\ &= \frac{1 - 2r + ((s - 1)\mathbb{T} - (s - 2))r^2}{1 - (\mathbb{T} + 2)r + 2r^2} \end{aligned}$$

and this verifies the induction step, concluding the proof of Proposition 6.3.

Acknowledgments. We thank the referee for their useful and constructive comments.

Funding. The first author acknowledges support from the Simons Foundation Collaboration Grant #625561 and thanks the University of Toronto for hospitality. The second author is partially supported by NSF grants DMS-1707882 and DMS-2104330, NSERC Discovery grant RGPIN-2018-04937, Accelerator Supplement grant RGPAS-2018-522593, and the Perimeter Institute for Theoretical Physics. The third author worked on parts of this project as a summer undergraduate research student at the University of Toronto.

References

- [1] K. Adiprasito, J. Huh, and E. Katz, Hodge theory for combinatorial geometries. *Ann. of Math. (2)* **188** (2018), no. 2, 381–452 Zbl [1442.14194](#) MR [3862944](#)
- [2] P. Aluffi and M. Marcolli, Feynman motives of banana graphs. *Commun. Number Theory Phys.* **3** (2009), no. 1, 1–57 Zbl [1171.81384](#) MR [2504753](#)
- [3] P. Aluffi and M. Marcolli, Algebro-geometric Feynman rules. *Int. J. Geom. Methods Mod. Phys.* **8** (2011), no. 1, 203–237 Zbl [1225.81101](#) MR [2782886](#)
- [4] P. Aluffi and M. Marcolli, Feynman motives and deletion-contraction relations. In *Topology of algebraic varieties and singularities*, pp. 21–64, Contemp. Math. 538, Amer. Math. Soc., Providence, RI, 2011 Zbl [1221.81076](#) MR [2777815](#)
- [5] P. Aluffi and M. Marcolli, A motivic approach to phase transitions in Potts models. *J. Geom. Phys.* **63** (2013), 6–31 Zbl [1264.14006](#) MR [2996396](#)
- [6] Y. André, An introduction to motivic zeta functions of motives. In *Motives, quantum field theory, and pseudodifferential operators*, pp. 3–17, Clay Math. Proc. 12, Amer. Math. Soc., Providence, RI, 2010 Zbl [1214.81094](#) MR [2762522](#)
- [7] A. Baratin, S. Carrozza, D. Oriti, J. Ryan, and M. Smerlak, Melonic phase transition in group field theory. *Lett. Math. Phys.* **104** (2014), no. 8, 1003–1017 Zbl [1297.81136](#) MR [3227703](#)
- [8] D. Bejleri and M. Marcolli, Quantum field theory over \mathbb{F}_1 . *J. Geom. Phys.* **69** (2013), 40–59 Zbl [1278.81130](#) MR [3040951](#)

- [9] J. Ben Geloun and R. Toriumi, Parametric representation of rank d tensorial group field theory: Abelian models with kinetic term $\sum_s |p_s| + \mu$. *J. Math. Phys.* **56** (2015), no. 9, paper no. 093503 Zbl [1322.83011](#) MR [3396221](#)
- [10] D. Benedetti, R. Gurau, and S. Harribey, Line of fixed points in a bosonic tensor model. *J. High Energy Phys.* **2019** (2019), no. 6, paper no. 053 Zbl [1416.81113](#) MR [3979830](#)
- [11] S. Bloch and P. Vanhove, The elliptic dilogarithm for the sunset graph. *J. Number Theory* **148** (2015), 328–364 Zbl [1319.81044](#) MR [3283183](#)
- [12] V. Bonzom, R. Gurau, A. Riello, and V. Rivasseau, Critical behavior of colored tensor models in the large N limit. *Nuclear Phys. B* **853** (2011), no. 1, 174–195 Zbl [1229.81222](#) MR [2831765](#)
- [13] V. Bonzom, R. Gurau, and V. Rivasseau, Random tensor models in the large N limit: uncoloring the colored tensor models. *Phys. Rev. D* **85** (2012), no. 8, paper no. 084037
- [14] V. Bonzom, V. Nador, and A. Tanasa, Diagrammatic proof of the large N melonic dominance in the SYK model. *Lett. Math. Phys.* **109** (2019), no. 12, 2611–2624 Zbl [1428.81115](#) MR [4029868](#)
- [15] S. Carrozza and A. Tanasa, $O(N)$ random tensor models. *Lett. Math. Phys.* **106** (2016), no. 11, 1531–1559 Zbl [1362.83010](#) MR [3555413](#)
- [16] V. I. Danilov and A. G. Khovanskij, Newton polyhedra and an algorithm for computing Hodge–Deligne numbers. *Math. USSR Izv.* **29** (1987), no. 2, 279–298 Zbl [0669.14012](#) MR [873655](#)
- [17] R. J. Duffin, Topology of series-parallel networks. *J. Math. Anal. Appl.* **10** (1965), 303–318 Zbl [0128.37002](#) MR [175809](#)
- [18] E. Fusy and A. Tanasa, Asymptotic expansion of the multi-orientable random tensor model. *Electron. J. Combin.* **22** (2015), no. 1, paper no. 1.52 Zbl [1310.81117](#) MR [3336566](#)
- [19] D. J. Gross and V. Rosenhaus, A generalization of Sachdev–Ye–Kitaev. *J. High Energy Phys.* **2017** (2017), no. 2, paper no. 093 Zbl [1377.81172](#) MR [3637521](#)
- [20] R. Gurau, Topological graph polynomials in colored group field theory. *Ann. Henri Poincaré* **11** (2010), no. 4, 565–584 Zbl [1208.81153](#) MR [2677739](#)
- [21] R. Gurau, The $1/N$ expansion of colored tensor models. *Ann. Henri Poincaré* **12** (2011), no. 5, 829–847 Zbl [1218.81088](#) MR [2802384](#)
- [22] R. Gurau, Colored group field theory. *Comm. Math. Phys.* **304** (2011), no. 1, 69–93 Zbl [1214.81170](#) MR [2793930](#)
- [23] R. Gurau, The complete $1/N$ expansion of a SYK-like tensor model. *Nuclear Phys. B* **916** (2017), 386–401 Zbl [1356.81180](#) MR [3611412](#)
- [24] R. Gurau, *Random tensors*. Oxford University Press, Oxford, 2017 Zbl [1371.81007](#) MR [3616422](#)
- [25] R. Gurau and J. P. Ryan, Colored tensor models – a review. *SIGMA Symmetry Integrability Geom. Methods Appl.* **8** (2012), paper no. 020 Zbl [1242.05094](#) MR [2942819](#)
- [26] J. Huh, Combinatorial applications of the Hodge–Riemann relations. In *Proceedings of the International Congress of Mathematicians – Rio de Janeiro 2018. Vol. IV. Invited lectures*, pp. 3093–3111, World Sci. Publ., Hackensack, NJ, 2018 Zbl [1448.05016](#) MR [3966524](#)

- [27] I. R. Klebanov and G. Tarnopolsky, Uncolored random tensors, melon diagrams, and the Sachdev–Ye–Kitaev models. *Phys. Rev. D* **95** (2017), no. 4, paper no. 046004
MR [3783911](#)
- [28] Yu. I. Manin and M. Marcolli, Moduli operad over \mathbb{F}_1 . In *Absolute arithmetic and \mathbb{F}_1 -geometry*, pp. 331–361, Eur. Math. Soc., Zürich, 2016 Zbl [1428.18035](#) MR [3701904](#)
- [29] M. Marcolli, *Feynman motives*. World Sci. Publ. Co. Pte. Ltd., Hackensack, NJ, 2010
Zbl [1192.14001](#) MR [2604634](#)
- [30] M. Marcolli and A. Port, Graph grammars, insertion Lie algebras, and quantum field theory. *Math. Comput. Sci.* **9** (2015), no. 4, 391–408 Zbl [1333.68172](#) MR [3426144](#)
- [31] M. Marcolli and G. Tabuada, Feynman quadrics-motive of the massive sunset graph. *J. Number Theory* **195** (2019), 159–183 Zbl [1403.14017](#) MR [3867438](#)
- [32] J. Riordan and C. E. Shannon, The number of two-terminal series-parallel networks. *J. Math. Phys. Mass. Inst. Tech.* **21** (1942), 83–93 MR [7511](#)
- [33] R. P. Stanley, Log-concave and unimodal sequences in algebra, combinatorics, and geometry. In *Graph theory and its applications: East and West (Jinan, 1986)*, pp. 500–535, Ann. New York Acad. Sci. 576, New York Acad. Sci., New York, 1989 Zbl [0792.05008](#)
MR [1110850](#)
- [34] A. Tanasa, Generalization of the Bollobás–Riordan polynomial for tensor graphs. *J. Math. Phys.* **52** (2011), no. 7, paper no. 073514 Zbl [1317.83038](#) MR [2848948](#)
- [35] E. Witten, An SYK-like model without disorder. *J. Phys. A* **52** (2019), no. 47, paper no. 474002 MR [4028950](#)

Communicated by Frédéric Patras

Received 22 July 2020.

Paolo Aluffi

Department of Mathematics, Florida State University, 208 Love Building, 1017 Academic Way, Tallahassee, FL 32306, USA; aluffi@math.fsu.edu

Matilde Marcolli

Department of Mathematics, California Institute of Technology, 1200 East California Boulevard, Pasadena, CA 91125, USA; matilde@caltech.edu

Waleed Qaisar

Department of Mathematics, University of Toronto, Bahen Centre, 40 St. George Street, Toronto, ON M5S 2E4, Canada; waleed.qaisar@mail.utoronto.ca